Optical and Quantum Electronics (2024) 56:661
https://doi.org/10.1007/s11082-023-06263-w

Sensitivity analysis on surface topography for laser-surface-texturing of Hastelloy C-276 superalloy: studies on micro-structure morphology characterization

Abhisekh Sen[1] · Debal Pramanik[2] · Nilanjan Roy[2] · Ahmed Mohammed Mahmood[3] · Partha Sarthi Ghosh[1] · Shubham Sharma[4,5,6] · Saja Hameed Kareem[7] · Changhe Li[7] · Hayder Sharif[8] · Mohamed Abbas[9]

Received: 25 August 2023 / Accepted: 30 December 2023 / Published online: 12 February 2024

Abstract
In the present scenario, controlling surface characteristics of superalloys such as friction, wear rates, and fatigue failure needs special attention for various manufacturing applications. The present research work deals with the analyses of a fiber laser surface texturing of Hastelloy C-276 to utilize the generated surfaces for high power applications. Texturing on Hastelloy C-276 surface has been achieved with the overlapping of linear micro-grooves. The effects of laser process parameters like laser power, scan speed, pulse frequency, and duty cycle on the surface morphology like arithmetic mean surface roughness (R_a), skewness (R_{sk}), and kurtosis (R_{ku}) have been studied. Empirical modeling of the process parameters for fiber laser surface texturing of Hastelloy C-276 has been carried out by response surface methodology. A sensitivity analysis is conducted here to find out the sensitivity of process variables on surface characteristics. The combination of laser power of 19.93 W, pulse frequency of 60 kHz, a duty cycle of 38.96%, and a scan speed of 8.41 mm/s lead to the optimized roughness criteria are 1.2 μm, − 0.35, and 3 for R_a, R_{sk}, and R_{ku} respectively.

Keywords Fiber laser · Surface texturing · Hastelloy · Roughness · Skewness · Kurtosis · Sensitivity analysis

1 Introduction

Presently, fabrication of micro-features or alternating the surface characteristics of difficult to machine materials have gained a tremendous interest to the researchers due to their excellent properties such as thermal resistance, wear resistance, corrosion resistance, etc. Various strategies are employed over to improve surface characteristics, e.g., electrochemical deposition, photolithography (Mohammed et al. 2017), etc. However, the aforesaid processes/strategies suffer considerably due to the slow processing time.

Over a wide range of surface texturing methods, laser surface texturing has become one of the emerging areas of surface engineering, evolved through the past decade with the modification of the surface topological characteristics. Besides, flexibility and

Extended author information available on the last page of the article

simultaneous reduction of time and cost during laser surface texturing have attributed to its popularity. Texturing of the surface quality of that workpiece needs to be carried out according to the required field of applications. The given material's tribological characteristics can be reduced or increased according to the manufacturing requirement through the laser surface texturing method. The process increases the load-carrying capacity of the material by improving the concentration and distribution of the developed stresses at the laser contact interface (Xing et al. 2013). Cross grooves, linear grooves, and dimple-shaped impressions are the most common procedures connected with the laser surface texturing process.

At present, nickel alloys are highly desirable in various manufacturing applications where high temperature and corrosion are involved. Hastelloy C-276 is also one of the preferred choices of material over other Hastelloy series materials in extreme environmental conditions due to its high molybdenum content and other superior properties (Davis 2000). The presence of low percentages of carbon in the alloy also restricts against precipitation of carbide during a laser welding process. As a result, corrosion-resistant welded structures are maintained throughout the process.

However, the aforesaid superior properties of Hastelloy C-276 have also contributed to the difficulty of attaining an excellent surface finish during machining of the alloy. As a result, several researchers have centralized their research on superalloys dealing with on aerospace industry (Al-Falahi et al. 2016). The amount of research works on Hastelloy C-276 is primarily limited to the laser welding method. Only a few researchers have tried to analyze the laser processing method on Hastelloy C-276 on the aspect of high-power applications. In this context, some of the research works have been highlighted to analyze the effects of different laser process parameters on laser surface texturing of Hastelloy C-276.

Ma et al. (2011) evaluated the mechanical properties as well as the microstructure of pulsed laser treatment on the nickel-based alloy. It was found that the micro-hardness of the treated region improved moderately due to the laser treatment, while the tensile strength decreased simultaneously due to the accumulation of dislocations. Laser surface modification of the nickel-based alloy was further carried out by Gordani et al. (2008). It was summarized that the laser-treated surface could provide better corrosion and pitting resistance compared to the untreated region. The effect of pulsed laser parameters on the nickel-based alloy's corrosion characteristics was further studied by Georges et al. (2006) to optimize the laser wavelength, energy, and time of interaction. It was concluded by the authors that to optimize the responses, heating, and melting phenomena should be governed and studied. Hasim et al. (2013) tried to improve the wear resistance of Hastelloy C-276 by laser surface treatment in an argon atmosphere. The primary consideration of this work was to identify optimum laser parameters at which wear-resistant surface can be obtained without the formation of a significant brittle phase that might degrade the inherent corrosion resistance. It was concluded that the microstructure of the laser-treated zone was greatly influenced by the laser power and scan speed.

From the previous studies, it can be summarized that only a few research works have concentrated to treat/modify Hastelloy C-276 surfaces predominantly for wear resistance. None of the research work was carried out to find out the optimized set of laser process parameters concerning surface characteristics. Thus, it is necessary to find out a cost-effective method to utilize Hastelloy C-276 with desired surface characteristics in high power applications and bearing applications.

In the present work, an effort has been carried out to analyze the effect of process parameters during laser-based surface texturing of Hastelloy C-276 with low power

CNC controlled fiber laser system. The responses are arithmetical mean surface roughness (R_a), skewness (R_{sk}) and kurtosis (R_{ku}). The R_a term provides a direct measure of the profile roughness, while, the others, R_{sk}, and R_{ku}, provide information about gloss and luster of the textured surface. The research aims to determine the effect of laser process parameters on these responses and obtain the desired surface topographical parameter values for the utilization of textured Hastelloy C-276 surface in various high-power applications. In the course of the design of experiments, a response surface methodology (RSM) is chosen, namely, the central composite design (CCD) method. CCD deals with four controllable factors: laser power, pulse frequency, duty cycle, and scan speed with five different levels. The analysis of variance (ANOVA) has been performed to analyze how the process parameters are affecting the fiber laser texturing process. The confirmations of the derived mathematical models are subsequently carried out. Finally, multi-objective optimization of the process parameters is also carried out to achieve desired surface roughness values. Five experiments are further carried out to determine the mean percentage error between predicted results and experimental results.

The intent of this investigation is to examine the surface characteristics of Hastelloy C-276 subsequent to the process of fibre laser surface texturing. The aim of this study is to utilise response surface methodology (RSM) in order to optimise the laser process parameters, including laser power, pulse frequency, duty cycle, and scan speed. The purpose is to attain specified surface roughness characteristics (Ra, Rsk, and Rku) that are suitable for high-power applications and bearings. The optimised parameters were determined as follows: a laser with a power rating of 19.93 W, a pulse with a frequency of 60 kHz, a duty cycle of 38.96%, and a scan speed of 8.41 mm/s. The significance of this work is in the cost-efficient and precise texturing of surface composed of Hastelloy C-276, thus enhancing their appropriateness for a wide range of applications, notably in high-power scenarios and bearing applications.

The rationale for doing this study is as follows, and in accordance with the surface characteristics control in Superalloys is concerned, Hastelloy C-276, serve an indispensable function for numerous industrial uses, wherein the attainment of controllable surface characteristics becomes imperative to ensure optimal performance in situations including friction, wear, and fatigue failure.

As far as novelty is concerned, the present investigation is distinguished by its emphasis on the optimisation of laser parameters for the process, notably targeting Hastelloy C-276, a material of paramount significance in high-power applications (Kibria et al. 2018; Watson and Spedding 1982; Lin et al. 2017). Prior research has not extensively investigated the optimal settings for laser-induced surface texturing of this specific material.

In context with the impact of processing parameters on surface characteristics are concerned, the authors have elucidated as follows,

Surface Roughness (R_a): Surface roughness, often known as R_a, refers to the measure of irregularities or deviations in the surface texture of a material. The sensitivity analysis conducted in the present research elucidated the complex relationship of laser power, scan speed, and surface roughness. The study presented in this work was to investigate the influence of laser power intensity, scan speed, and assist gas pressure on the surface roughness. The impact of these parameters was evaluated through the use of ANOVA and sensitivity plots, which are apparent in the mentioned below sections, respectively.

Surface Skewness (R_{sk}): The analysis of the surface skewness, denoted as R_{sk}, yielded valuable information about the surface's capacity to retain fluid along with its bearing characteristics. The parameters of laser power and scan speed were determined to be significant

factors that influence the skewness of the surface, as depicted in the mentioned below section.

Surface Kurtosis (R_{ku}): The investigation of surface kurtosis (R_{ku}) examined the impact of factors including scan speed and pulse frequency on the textural characteristics of the surface, namely its spiky or bumpy nature or appearance form. The research provided insight on the significance of thermal profiles, hydrodynamic waves, and energy density on surfaces morphology, illustrated in the mentioned below section.

The process of optimisation and validation is a crucial aspect of scientific study.

In order to attain the desired surface roughness values, a multi-objective optimisation approach was employed. The experimentally validated optimised parameters demonstrated a substantial degree of agreement among the predicted and experimental values, as illustrated by the mentioned below sections.

The confirmatory tests were conducted to validate the optimised parameters and examine the reliability, accuracy, dependability, and precision of the models. The findings of these experiments demonstrated minimal prediction errors, specifically within a range of 5%, for the parameters R_a, R_{sk}, and R_{ku}. This outcome offers additional evidence corroborating an accuracy as well as reliability of our models.

The foremost target of this research aimed to explore the feasibility of employing fibre laser surface texturing as a cost-effective/economical, and precise technique for modifying the surface characteristics of Hastelloy C-276. The target of this research was to optimise the surface roughness variables, namely Ra, Rsk, and Rku, to particular values of 1.2 µm, − 0.35, and 3, respectively. This optimisation was aimed at ensuring the suitability of the surfaces for application in high-power systems and bearings. Through a rigorous experimental setup and analysis, researchers attempted to find the optimal set of processing parameters including laser power, pulse frequency, duty cycle, and scan speed. The study additionally aimed to provide a comprehensive understanding of the influence of these factors on the surface characteristics of Hastelloy C-276, thus enhancing its applicability in diverse applications in engineering. Furthermore, researchers conducted confirmatory tests to evaluate the optimised parameters and highlighted the efficacy of the suggested technique.

Additionally, the investigation of surface roughness characteristics has considerable significance as it directly impacts the performance and behaviour of materials across diverse applications. The management of surface characteristics is of paramount significance in optimising wear resistance, minimising friction, and mitigating fatigue failure in high-power systems and bearings, particularly in the context of Hastelloy C-276, an alloy composed of nickel, molybdenum, and chromium. Surface texturing, although it necessarily causes a rise in roughness, enables meticulous control of these roughness characteristics. By effectively optimising the factors related to surface roughness, an optimal balance is attained, wherein the enhanced roughness is efficiently balanced with the necessitate surface characteristics.

Moreover, the study's influence has enormous significance. The utilisation of optimised surface characteristics causes enhanced fluid retention and lubricating capabilities, primarily attributed to the existence of negative skewness. Consequently, the material exhibits suitability for various bearing applications. In addition, the optimised parameters employed in the present investigation have culminated in specified roughness values (Ra = 1.2 µm, Rsk = − 0.35, Rku = 3) that are specifically tailored to high-power applications. These values are crucial in ensuring the surface exhibits the requisite characteristics for efficient functioning operation. This research not only enhances the foundational comprehension of the laser surface texturing method nevertheless offers valuable insights into customising

material surfaces for certain applications in industry. The findings of this study offer an outline for the potential application of Hastelloy C-276 across multiple engineering industries, therefore meeting the requirement for materials that possess controlled surface characteristics.

In summary, this study provides a comprehensive understanding of the significance of surface roughness parameters, particularly in the context of surface texturing techniques, and highlights their crucial influence on material performance. By attaining meticulous manipulation for these factors, researchers have unveiled the inherent capabilities of Hastelloy C-276 in high-power systems and bearings, therefore exerting a substantial influence on the domain of materials research and engineering.

All in all, the purpose of this research is to examine the effect of fiber laser surface texturing on Hastelloy C-276 and to determine how various laser process parameters affect the surface characteristics, namely the arithmetic mean surface roughness (R_a), skewness (R_{sk}), and kurtosis (R_{ku}). Despite the fact that surface texturing tends to enhance surface roughness, this research seeks to identify the optimal laser process parameters for achieving the desired surface roughness values for high-power applications.

This study's significance lies in its contribution to surface texturing of Hastelloy with low power nano second pulsed laser system. Researchers and manufacturers can optimize the surface properties of Hastelloy C-276 for specific applications if they comprehend the relationship between laser process parameters and surface characteristics. In automotive, solar power, and optical chamber applications where Hastelloy C-276 is used, this can result in enhanced performance, including reduced friction, wear rates, and fatigue failure (Soveja et al. 2008; Yilbas and Ali 2016; Horváth et al. 2015). In addition, the findings of this study can lead to more cost-effective methods for employing Hastelloy C-276 in high-power applications, which will benefit industries that rely on the material's superior properties, such as thermal resistance, abrasion resistance, and corrosion resistance. This study also seeks to address the difficulty of regulating the surface characteristics of superalloys, specifically Hastelloy C-276, by means of fiber laser surface texturing. By examining the effect of laser process parameters on surface roughness and other characteristics, this research offers valuable insights into optimizing surface properties for a variety of manufacturing applications.

2 Materials and methods

The contextualization of the research work is achieved through a comparative study with results obtained from previous literature (Sarker et al. 2018; Roy and Manna 2001; Guarino et al. 2018). Previous studies have investigated the impact of chemical etching and mechanical polishing techniques on the surface properties of Hastelloy C-276. In this present research work, Hastelloy C-276 is having a dimension of 50 mm × 50 mm × 1 mm of thickness has been selected for the analysis of considered process parameters on the responses. Before the fiber laser surface texturing, Hastelloy C-276 surface is cleaned with an ultrasonic cleaner. The surface characteristics for the untreated surface of Hastelloy C-276 are R_a of 19.6 nm, R_{sk} of -0.0698, and R_{ku} of 2.90. The microscopic view of the untreated Hastelloy C-276 surface is shown in Fig. 1 at 10× magnifications. Later 50-W multi-diodes pumped fiber laser system is utilized to generate textured surfaces on Hastelloy C-276 in different machining conditions. The working wavelength is 1064 ± 10 nm. The laser beam is collimated and subsequently bent through a 100% reflecting mirror, which is placed at an

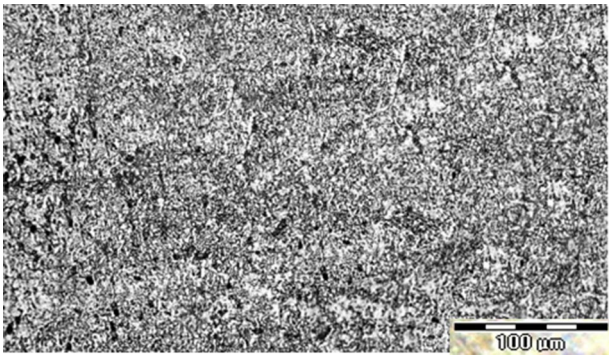

Fig. 1 Microscopic view of an untreated surface of Hastelloy C-276

angle of 45° with the horizontal plane. After that, the laser beam is focused on the targeted surface through an F-θ lens. The measured spot diameter of the fiber laser beam is found to be approximately 21 µm.

The untreated surface of Hastelloy C-276 is treated with multiple overlapped micro-grooves for modifying the surface characteristics. Repetition of multiple laser micro-grooves is selected as the fabrication method of textured regions on the workpiece surface. During laser irradiation on the workpiece surface at high temperatures, localized melting leads to material removal from the heated surface (Yilbas and Ali 2016; Griffiths 2001).

In the present setup, Hastelloy C-276 is placed on a workpiece table to move in X and Y directions with relative motion. The length of a micro-groove is set at 5 mm. A total number of 250 micro-grooves is made with a transverse overlap distance of 7 µm between each other. During the trial runs, it was observed that as the distance between the two micro-grooves (at Y direction) is lowered, the overlap between two continuous micro-grooves is increased notably. 7 µm is the lowest transverse feed for the present fiber laser system due to the system limitation. Equation 1 deals with the correlation between transverse feed and transverse overlap factor (Kibria et al. 2018; Dwivedi et al. 2023; Cui et al. 2022a). Mohammed et al. (2017) derived that pulse overlap and pulse frequency has a significant effect on the surface roughness characteristics.

From Eq. 1, the transverse overlap percentage is measured as 66.67% for the distance between two consecutive grooves of 7 µm. The combination of 250 micro-grooves and a transverse feed of 7 µm results in a square area of 5×5 cm^2. The depth increment of the textured region is not conceived as the principal criterion of the present research study. Thus, the number of repetitions of the grooves is kept constant at 2. During the trial runs, the effect of assist air is found useful only at high pressure for which the assist air pressure

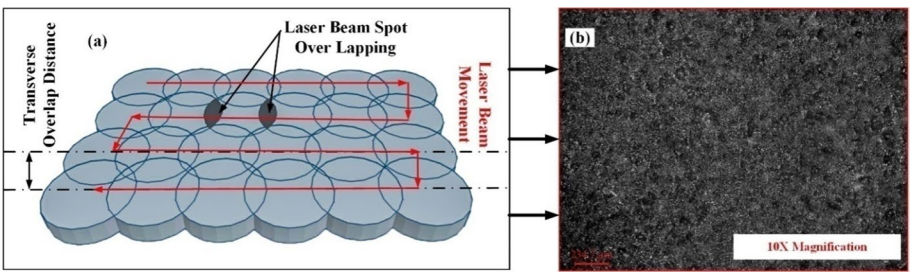

Fig. 2 **a** Schematic representation of the laser surface texturing process; **b** formation of the textured surface

is kept constant at 4 kgf/cm^2. The schematic representation of the laser texturing process and the textured region's formation is shown in Fig. 2a, b, respectively.

A photographic view of various fiber laser-generated textured surfaces is shown in Fig. 3.

$$\text{Transverse Overlap} = \frac{\text{Laser Spot Diameter at foused condition} - \text{Transverse overlap distance}}{\text{Laser Spot Diameter at foused condition}} \times 100\% \quad (1)$$

2.1 Experimental planning

The present investigation has been designed to utilize the central composite blocked design (CCD) of experiments, incorporating four factors. The experimental analyses have been carried out utilizing Minitab 17. A total of 31 experiments have been conducted, each of which has been replicated three times. The selection and range of each process parameter are determined through empirical experimentation. In the present context, the experimental analysis has been conducted using a range of laser process parameters. Specifically, the laser power was varied between 10 and 20 W, the pulse frequency ranged from 60 to 80 kHz, the duty cycle varied from 30 to 70%, and the scan speed was set between 1 and 9 mm/s. Table 1 provides the specified range of individually controllable process parameters achieved through the utilization of the Response Surface Method (RSM) technique. According to Watson and Spedding (1982), when examining a textured surface profile, it is essential to consider the height and spacing characteristics of the surface irregularities. The instructive parameters for analyzing a surface profile were demonstrated by Lin et al. (2017) to be R_{sk} and R_{ku}. However, it is

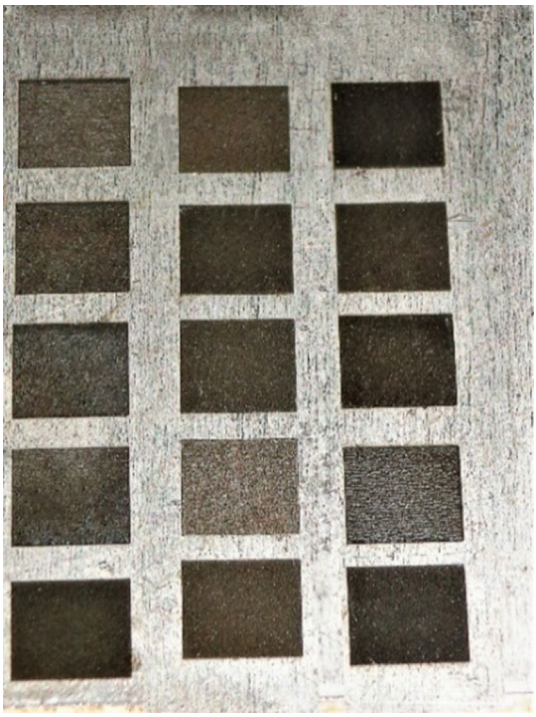

Fig. 3 Photographic view of the fiber laser textured surfaces on Hastelloy C-276

Table 1 Process parameters and its range

Controllable parameters	Units	Levels				
		− 2	− 1	0	1	2
Power setting (X_1)	Watt	10	12.5	15	17.5	20
Pulse frequency (X_2)	kHz	60	65	70	75	80
Duty cycle (X_3)	%	30	40	50	60	70
Scan speed (X_4)	mm/s	1	3	5	7	9

necessary to consider R_a in conjunction with the other two roughness criteria in order to assess the geometric characteristics of the textured surface (Liu et al. 2023; Jia et al. 2022; Cui et al. 2022b). The current analysis focuses on the consideration of R_a, R_{sk}, and R_{ku} for the laser-textured square profiles. The skewness parameter plays a significant role in the regulation of wear and the bearing surface (Singh et al. 2022b; Khan et al. 2022; Duan et al. 2022). Kurtosis is a fundamental parameter used in characterizing the surface roughness of a profile, specifically in terms of the sharpness of its probability density (Syreyshchikova et al. 2021a; Singh et al. 2022a). Figure 4 is a flowchart illustrating the research technique employed in this study.

2.2 Measurements

The surface roughness criteria R_a, R_{sk}, R_{ku}, have been measured by Mitutoyo SJ 410 surface roughness tester with a Gaussian filter. The responses are calculated under the ISO 4287:1997 standard. The measurements are repeated at five reference lines, and the result is the average of these values. Talysurf CCI non-contact surface profiler system is also utilized to show the 3D profiles of the laser textured surfaces as well as their corresponding roughness profiles.

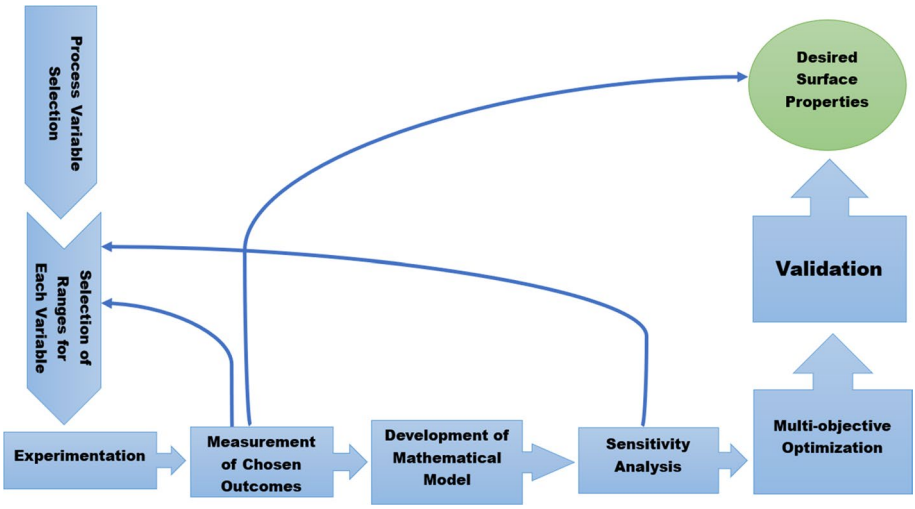

Fig. 4 Flowchart of the research methodology for the current work

3 Results and discussions

Table 2 presents the experimental design and the corresponding observed results. Statistical analyses were performed to validate the mathematical models of responses based on the results of laser surface texturing on Hastelloy C-276. Mathematical models are formulated with the purpose of establishing a correlation between process parameters and performance criteria.

Table 3 displays the outcomes of the analysis of variance (ANOVA) conducted on the variables R_a, R_{sk}, and R_{ku}. The findings encompass the degrees of freedom (DOF), F-value,

Table 2 Experimental design and observed values of responses

Exp. no.	Process parameters				Responses		
	Laser power (W)	Pulse frequency (kHz)	Duty cycle (%)	Scan speed (mm/s)	R_a (μm)	R_{sk}	R_{ku}
1	15.0	70	50	5	6.25	0.28	2.91
2	17.5	65	40	3	9.13	0.42	3.77
3	17.5	75	40	7	6.22	0.3	2.25
4	15.0	70	50	5	6.43	0.21	2.92
5	12.5	75	60	7	5.16	0.1	1.35
6	15.0	70	50	5	6.40	0.28	2.95
7	15.0	70	50	9	5.08	0.11	1.65
8	17.5	75	40	3	7.92	0.23	2.65
9	15.0	70	50	5	5.98	0.23	2.93
10	15.0	70	50	5	5.88	0.28	2.92
11	12.5	75	60	3	4.08	0.16	2.73
12	15.0	70	50	5	6.25	0.27	2.78
13	15.0	70	70	5	5.48	0.53	2.57
14	12.5	65	60	7	2.99	− 0.22	1.46
15	15.0	70	50	5	5.99	0.27	2.80
16	17.5	65	60	7	5.69	0.07	2.27
17	12.5	75	40	3	5.01	− 0.21	2.38
18	10.0	70	50	5	2.86	− 0.33	2.29
19	17.5	65	40	7	4.04	0.18	2.97
20	17.5	65	60	3	9.92	0.28	2.92
21	15.0	60	50	5	5.52	− 0.19	2.34
22	12.5	65	60	3	3.99	0.27	2.91
23	15.0	70	50	1	8.66	0.49	3.54
24	15.0	80	50	5	7.01	− 0.03	1.16
25	12.5	75	40	7	4.62	− 0.14	1.22
27	17.5	75	60	3	8.44	0.31	2.39
28	12.5	65	40	3	5.10	0.11	3.09
29	20.0	70	50	5	8.71	0.17	3.31
30	17.5	75	60	7	7.95	0.43	1.73
31	12.5	65	40	7	2.13	− 0.22	1.92

Table 3 Analysis of variance (ANOVA) for response surface quadratic model of R_a, R_{sk}, and R_{ku}

Source	DOF	R_a		R_{sk}		R_{ku}	
		F-value	*p* value	F-value	*p* value	F-value	*p* value
Model	14	104.02	0.000	58.89	0.000	97.55	0.000
Linear	4	288.44	0.000	96.94	0.000	243.09	0.000
Laser power	1	807.62	0.000	267.04	0.000	149.34	0.000
Pulse frequency	1	49.60	0.003	9.28	0.008	207.17	0.001
Duty cycle	1	26.11	0.000	31.84	0.000	55.89	0.000
Scan speed	1	270.42	0.000	79.62	0.000	559.96	0.003
Square	4	17.81	0.000	72.66	0.000	70.63	0.000
2-Way Interaction	6	38.55	0.000	24.35	0.000	18.48	0.000
Lack-of-fit	10	1.87	0.229	2.54	0.133	2.77	0.112
Model summary		R^2-98.91%, R^2 (Adjusted)-97.96%, R^2 (Predicted)-94.90%		R^2-98.10%, R^2 (Adjusted)-96.43%, R^2 (Predicted)-90.63%		R^2-98.84%, R^2 (Adjusted)-97.83%, R^2 (Predicted)-94.24%	

and p-value. The p-values associated with the lack of fit of the models for responses R_a, R_{sk}, and R_{ku} width at a 95% confidence level are 0.229, 0.133, and 0.112, respectively. The determination of the significance of process variables is typically based on the p-value obtained from the ANOVA, which is also employed in this study (Aggarwal et al. 2020; Syreyshchikova et al. 2021b; Singh et al. 2022c). The *p* values of the selected variables are less than 0.05, suggesting that there is no significant lack of fit. Therefore, the second-order polynomial model that has been developed is statistically significant and has been appropriately fitted to the entire machining outcome. Furthermore, the justification for all the developed models is supported by the closer proximity of the R^2, R^2 (adjusted), and R^2 (predicted) values to 1. The model's validation has been confirmed by the negligible value of S observed for all the responses. The developed models for R_a, R_{sk}, and R_{ku} demonstrate sufficient statistical adequacy in predicting the responses. The backward elimination method is utilized in this study to eliminate the irrelevant terms identified during the ANOVA for all three responses. This approach aims to enhance the relevance of the developed model. The models that have been developed are presented in this document.

$$\begin{aligned} Ra = {} & -31.1 + 3.291\,X_1 + 0.356\,X_2 + 0.042\,X_3 - 2.703\,X_4 - 0.02088\,X_1^2 - 0.00042\,X_2^2 \\ & - 0.003189\,X_3^2 - 0.0261\,X_4^2 - 0.03035\,X_1 * X_2 + 0.01373\,X_1 * X_3 - 0.1296\,X_1 * X_4 \\ & - 0.00024\,X_2 * X_3 + 0.04769\,X_2 * X_4 + 0.02084\,X_3 * X_4 \end{aligned} \tag{2}$$

$$\begin{aligned} R_{sk} = {} & -13.44 + 0.4135X_1 + 0.3999X_2 - 0.0834X_3 - 0.7740X_4 - 0.01377X_1^2 - 0.003742X_2^2 \\ & + 0.000421X_3^2 + 0.00224X_4^2 + 0.001750X_1 * X_2 - 0.002025X_1 * X_3 + 0.00687X_1 * X_4 \\ & + 0.001138X_2 * X_3 + 0.00919X_2 * X_4 - 0.000656X_3 * X_4 \end{aligned} \tag{3}$$

$$\begin{aligned} R_{ku} = {} & -53.37 + 0.835X_1 + 1.5465X_2 - 0.0155X_3 - 0.581X_4 - 0.00491X_1^2 - 0.011726X_2^2 \\ & - 0.000793X_3^2 - 0.02048X_4^2 - 0.00675X_1 * X_2 - 0.005775X_1 * X_3 + 0.03487X_1 * X_4 \\ & + 0.002538X_2 * X_3 + 0.00206X_2 * X_4 - 0.002344X_3 * X_4 \end{aligned} \tag{4}$$

3.1 Influence of process parameters on the surface roughness criteria

Response surfaces have been generated by plotting the relationship between one process criterion and two process parameters at a time, while the remaining two process parameters are held constant. With the aid of sensitivity analysis, the results of parametric analyses on R_a, R_{sk}, and R_{ku} have been studied in detail, taking into account process variables like, laser power, pulse frequency, duty cycle, and scan speed. Equations 2, 3, and 4 are partially differentiated with respect to four specific process variables in order to determine the sensitivity of machining outcomes.

3.1.1 Sensitivity of surface roughness (R_a)

$$\delta R_a/\delta X1 = 3.291 + 0.04176X_1 - 0.03035X_2 + 0.01373X_3 - 0.01296X_4 \quad (5)$$

$$\delta R_a/\delta X2 = 0.356 - 0.00084X_2 - 0.03035X_1 - 0.00024X_3 + 0.04769X_4 \quad (6)$$

$$\delta R_a/\delta X3 = 0.042 - 0.006378X_3 + 0.01373X_1 - 0.00024X_2 + 0.02084X_4 \quad (7)$$

$$\delta R_a/\delta X4 = -2.703 - 0.0522X_4 - 0.1296X_1 + 0.04769X_2 + 0.02084X_3 \quad (8)$$

Figure 5 illustrates the relationship between surface roughness and the selected process variables, highlighting their sensitivity. The data reveals that there is a positive correlation between laser power and pulse frequency across all levels, indicating heightened sensitivity. Conversely, scan speed exhibits a negative correlation, suggesting a decrease in sensitivity (Cui et al. 2023; Xu et al. 2022; Singh et al. 2023a). The sensitivity of the duty cycle exhibits a positive relationship up to the lower threshold but demonstrates a negative association with further increases in levels (Prasanthi et al. 2023; Sun et al. 2023; Kumar et al. 2023a). The sensitivity of surface roughness may be attributed to the underlying physical mechanism of inhomogeneous energy deposition, which is influenced by pulse frequency (Kiranakumar et al. 2022; Shahid et al. 2022). Additionally, it can be noted that

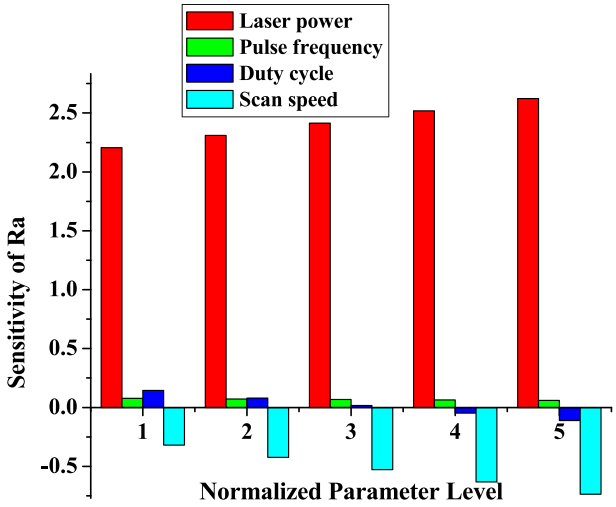

Fig. 5 Sensitivity plot for surface roughness (R_a)

the sensitivity of laser power and scan speed is higher compared to the other two process variables. This observation is supported by the ANOVA result for R_a. The dynamics of the melt pool have a significant impact on the quality of the surface. The presence of assist gas at moderate pressure leads to a decrease in the viscosity of the melt pool, thereby increasing the likelihood of undesired solidification (Kumar et al. 2023b; Khan et al. 2023). Consequently, this results in an increase in surface roughness.

The laser-material interaction time is significantly reduced when employing a high scan speed in comparison to a low scan speed. This decrease in interaction time limits heat transfer and allow the material to melt and solidify quickly. As a result, both the surface quality and surface roughness improve. In addition, the high scan speed reduces the likelihood of material overheating and thermal damage, further enhancing the surface quality. In order to achieve high-quality surfaces during laser melting processes, it is essential to regulate the scan speed and use assist gas at the proper pressure (Soveja et al. 2008). Thus, decrement in MRR occurs. Besides, when the scanning speed is increased, there is a significant reduction in the quantity of molten material. R_a values show a decrease in surface roughness, which is consistent with the limited amount of molten material present those results from combining high scan speeds with low pulse frequencies (Singh et al. 2023b; Kumar et al. 2023c; Sehar et al. 2022). Consequently, there is a significant enhancement in the homogeneity of the textured surface.

Figure 6 illustrates a microscopic examination of a fiber laser textured surface observed at a magnification of 50×. The surface exhibits a uniformly distributed, textured profile. When the laser power is increased to a high level, the material of the textured surface acquires a significant amount of energy, leading to a rapid melting process. The spot center of laser irradiation is where the maximum peak power intensity is attained, which can be attributed to the Gaussian mode of distribution exhibited by the fiber laser beam (Yilbas and Ali 2016). This melting process results in the formation of a molten pool at the spot center, surrounded by a solidified rim. The molten pool has a smooth and glossy appearance, indicating the complete melting and solidification of the material. The solidified rim, on the other hand, retains the textured profile of the original surface but with a pronounced and defined pattern. Following the occurrence, there is a gradual reduction in power density as one move closer to the periphery of the irradiated area. Consequently, the occurrence of melting is observed at the periphery of the irradiated spot, in conjunction with evaporation taking place at the center of the spot. The aforementioned phenomena result in

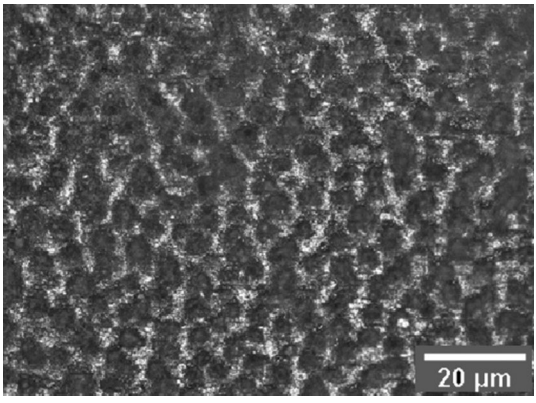

Fig. 6 Microscopic view of fiber laser textured surface

increased irregularities on the textured surface when subjected to texturing with a nanosecond pulsed fiber laser operating at higher levels of laser power (Dikshit et al. 2023; Lashin et al. 2022; Vemanaboina et al. 2023).

The angle of indentation, beam structure, and overlapping of two consecutive travel paths are fixed at 90° along with the Gaussian beam is at 66.67%. In Fig. 7a, the effect of thermal energy in terms of laser power in association with irradiation time is illustrated in the form of a surface plot. It is evident from the plot that a lower value of surface roughness (R_a) may be achieved at a lower value of laser power with a higher value of scan speed. The aforesaid parametric settings help to achieve adequate energy fluence via multi-photon absorption to remove material from the line of laser beam travel. In this experimental study, the material removal mechanism may be governed by the pyrolithic process; energy density per unit time is the most important factor for uniform ablation, as also shown by the contour plot. To better understand the effect of the second-order interactions in each texturing response, contour plots of the developed mathematical models are presented in Fig. 7b, c.

3.1.2 Sensitivity analysis of skewness (R_{sk})

$$\delta R_{sk}/\delta X1 = 0.4135 - 0.0274X_1 + 0.001750X_2 - 0.002025X_3 + 0.00687X_4 \quad (9)$$

$$\delta R_{sk}/\delta X2 = 0.3999 - 0.007484X_2 + 0.001750X_1 + 0.001138X_3 + 0.00919X_4 \quad (10)$$

$$\delta R_{sk}/\delta X3 = -0.0834 + 0.000842X_3 - 0.002025X_1 + 0.001138X_2 - 0.000656X_4 \quad (11)$$

$$\delta R_{sk}/\delta X4 = -0.7740 + 0.00448X_4 + 0.00687X_1 + 0.00919X_2 - 0.00656X_3 \quad (12)$$

According to the study (Horváth et al. 2015), the surface that exhibits a negative skewness possesses superior fluid retention capability and bearing properties. Therefore, improved surface performance can be attained by ensuring that the surfaces possess negative skewness values (Sarker et al. 2018). Based on the findings presented in Fig. 8, it can be observed that the variable with the greatest sensitivity to skewness is the laser power. The surface exhibits crater and rippled profiles when subjected to laser-based irradiation, resulting from the uneven distribution of laser energy (Al-Tameemi et al. 2021; Singh et al. 2022d, 2023c). This uneven energy distribution induces Marangoni-driven flow and capillary waves, ultimately leading to re-solidification. Therefore, the laser power is the most sensitive variable. The impact of alterations in the thermal profile of a melt pool extends beyond the modification of the thermal diffusivity and dynamic viscosity of the molten material. These changes also give rise to hydrothermal waves that induce surface tractions perpendicular to the orientation of ripples.

The scan speed exhibits greater sensitivity at lower values compared to higher values. The thermo-capillary flow mechanism resulting from a temperature gradient is the primary factor influencing changes in surface morphology during the processing of materials using nanosecond pulse lasers. The sensitivity of the pulse frequency exhibits a positive trend up to a certain threshold, beyond which it becomes negatively sensitive. The utilization of low laser power, in conjunction with a duty cycle of 55%, results in the generation of profiles exhibiting negative skewness. The increase in laser power leads to the presence of textured surfaces, which exhibit favorable skewness profiles.

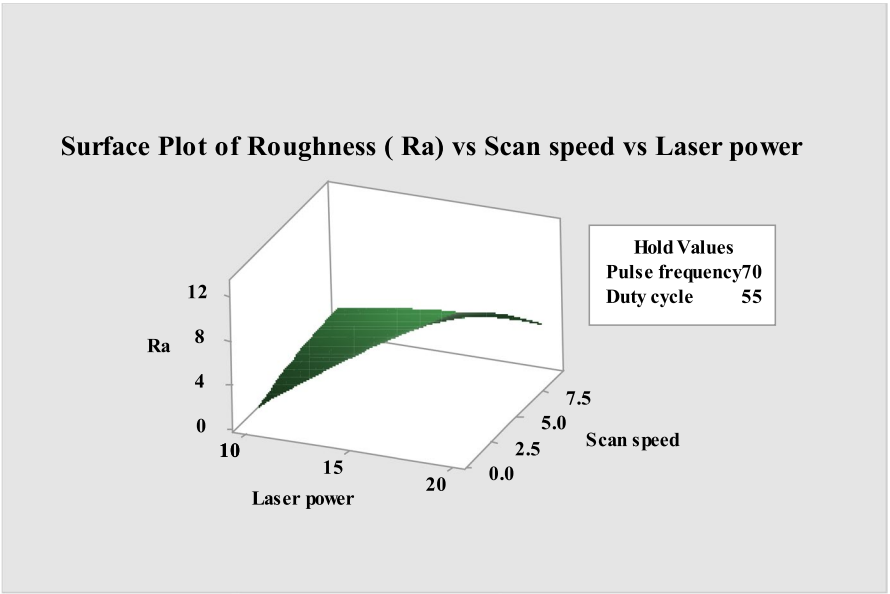

(a) Surface plot for surface roughness (Ra) vs laser power & scan speed

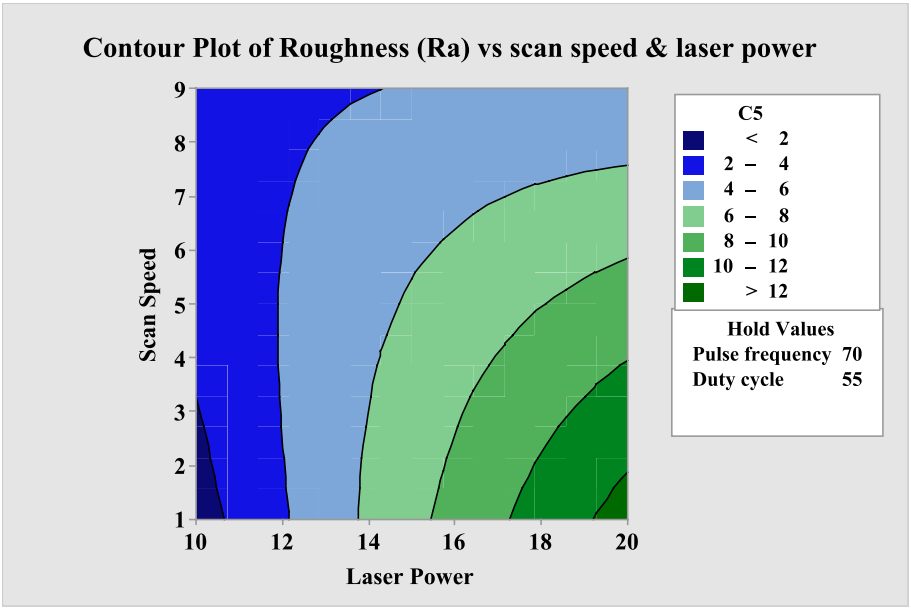

(b) Contour plot for surface roughness (Ra) vs laser power & scan speed

Fig. 7 **a** Surface plot for surface roughness (R_a) versus laser power and scan speed. **b** Contour plot for surface roughness (R_a) versus laser power and scan speed. **c** Residual plots for surface roughness (R_a)

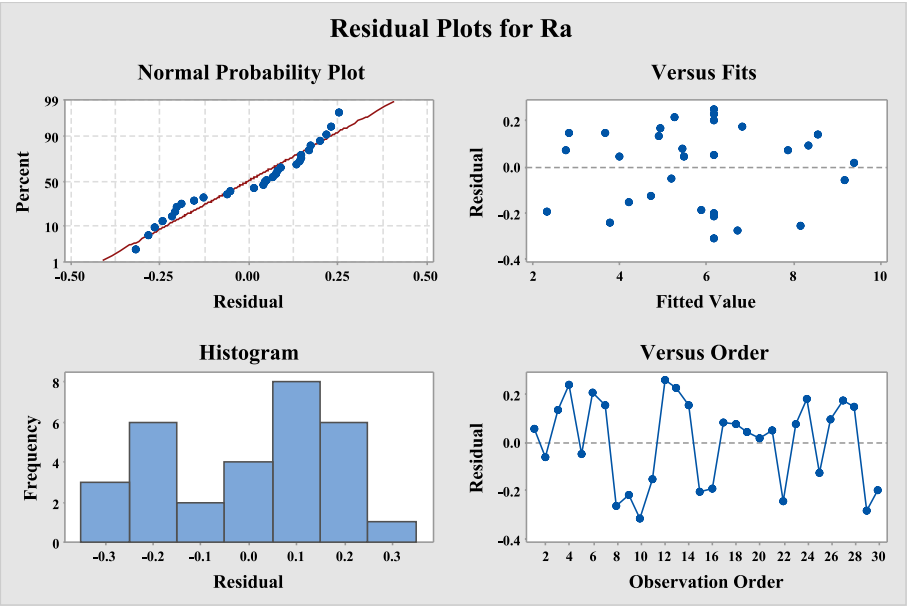

(c) Residual plots for surface roughness (R_a)

Fig. 7 (continued)

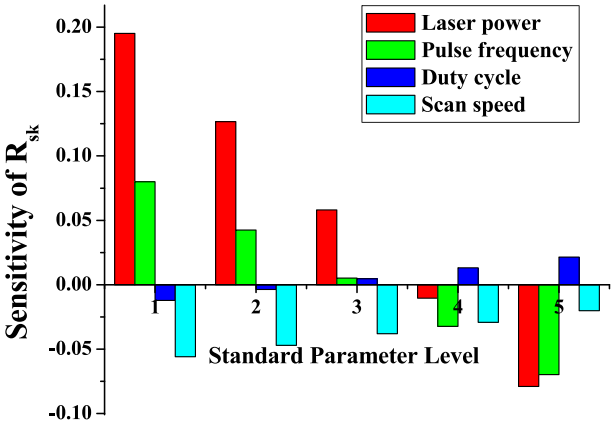

Fig. 8 Sensitivity plot for surface skewness (R_{sk})

During the process of pulsed fiber laser surface texturing on Hastelloy C-276, the temperature experiences rapid oscillations as a result of the alternating states of the laser being on and off within a complete repetitive pulse cycle. Consequently, the thermal gradient within the zone of surface texturing is substantial. A homogeneous grain structure can be achieved by utilizing a low duty cycle when applying texturing using a pulsed-mode, low power fiber laser. Moreover, when the surface is subjected to high laser power, the asperities experience yielding, resulting in a modified profile. The increase in laser power leads to the restructuring of asperities on the textured surface (Roy and Manna 2001). At elevated laser power levels, it is observed that textured surfaces exhibit greater peak

heights compared to their corresponding valleys. This phenomenon can be attributed to the increased melting of material followed by rapid solidification, which is facilitated by the presence of an assist gas at a specific pressure. Therefore, it can be observed that high laser power leads to favorable skewness profiles.

The surface plot demonstrates that alterations in laser power and scan speed have an impact on surface skewness (R_{sk}). It has also been found that the needed surface symmetry, specifically lowering the R_{sk} value, can be reached by using a faster scan speed and a lower laser intensity during the texturing process. Some of the above parametric configurations can include enough laser energy density at the texturing zone to make it easier to remove the same amount of material along the whole path in almost no time. The desired outcome of the reduced interaction period between the laser beam and workpiece is the occurrence of anti-adhesive effects on the produced surface. The contour map depicted in Fig. 9a–c provides further evidence supporting the aforementioned phenomenon.

3.1.3 Sensitivity analysis on Kurtosis (R_{ku})

$$\delta R_{ku}/\delta X_1 = 0.835 - 0.00982X_1 - 0.00675X_2 - 0.005775X_3 + 0.03487X_4 \quad (13)$$

$$\delta R_{ku}/\delta X_2 = 1.5465 - 0.023452X_2 - 0.00675X_1 + 0.002538X_3 + 0.00206X_4 \quad (14)$$

$$\delta R_{ku}/\delta X_3 = -0.0155 - 0.001586X_3 - 0.005775X_1 + 0.002538X_2 - 0.002344X_4 \quad (15)$$

$$\delta R_{ku}/\delta X_4 = -0.581 - 0.04096X_4 + 0.03487X_1 + 0.00206X_2 - 0.002344X_3 \quad (16)$$

The laser texturing process satisfies the criteria outlined in the central limit theorem of statistics (Griffiths 2001), wherein the occurrences are abundant, stochastic, and cumulative. When the kurtosis value of the analyzed surface is elevated, it is classified as exhibiting a spiky characteristic. A surface is classified as having a bumpy texture when its kurtosis value is low. According to Fig. 10, the scan speed is the most sensitive process variable, followed by pulse frequency, laser power, and duty cycle. The observation reveals that there is a positive sensitivity to pulse frequency up to a certain midpoint, after which it becomes negatively sensitive. Conversely, the sensitivity of R_{ku} for scan speed is consistently negative. The observed phenomenon is attributed to the limited depth of laser beam penetration at elevated pulse frequencies. Furthermore, it should be noted that the level of randomness in the surface profile increases at lower pulse frequencies, regardless of the specific value of the duty cycle. Nevertheless, an increase in pulse frequency leads to a decrease in the value of kurtosis. The observed profiles exhibit a Gaussian distribution, indicating that the treated surfaces offer enhanced management of wear and friction compared to the untreated region (Guarino et al. 2018). It is widely recognized that the primary factor contributing to the formation of micro spikes at the fusion zone of a laser-treated region is the induction of hydrodynamic waves caused by Marangoni shear-generated convection. The relationship between the duration of irradiation and the speed of scanning, combined with the repetition rate, primarily determines the pulse energy density at the specific area being irradiated. The generation of transverse counter-rotating rolls is affected by the instability of hydrodynamics at higher pulse frequencies, leading to an increased formation of micro spikes. The decrease in scanning speed, in conjunction with a decrease in laser power, results in a notable increase in the kurtosis of the surfaces. When the scan speed and laser power are set to their minimum values, the kurtosis value surpasses the range expected for a Gaussian

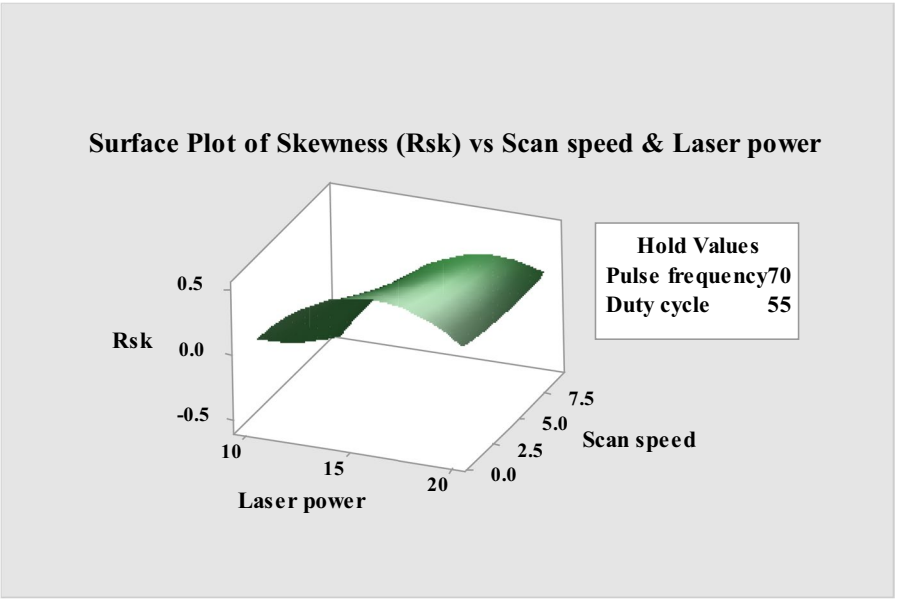

(a) Surface plot for surface skewness (R_{sk}) vs laser power & scan speed

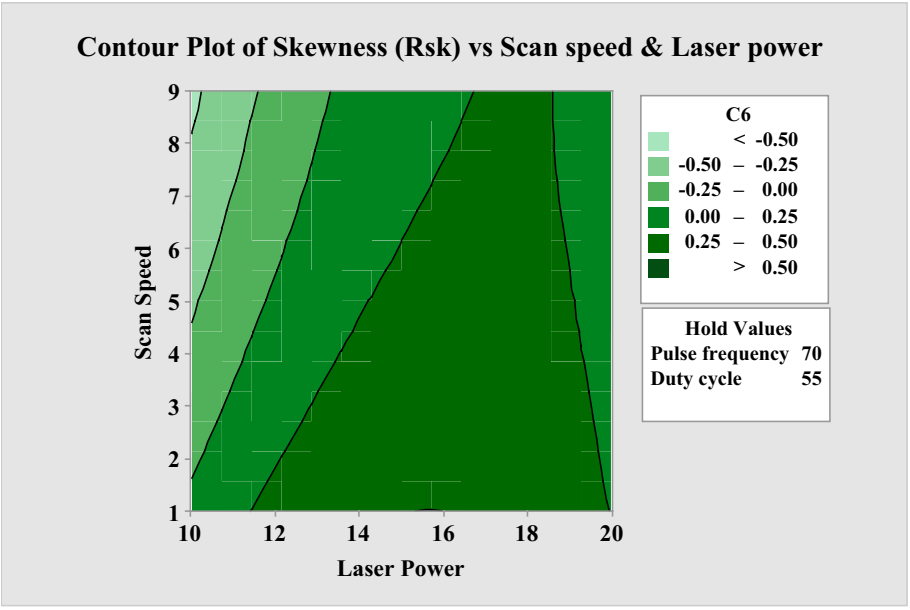

(b) Contour plot for surface skewness (R_{sk}) vs laser power & scan speed

Fig. 9 **a** Surface plot for surface skewness (R_{sk}) vs laser power and scan speed. **b** Contour plot for surface skewness (R_{sk}) vs laser power and scan speed. **c** Residual plots for surface skewness (R_{sk})

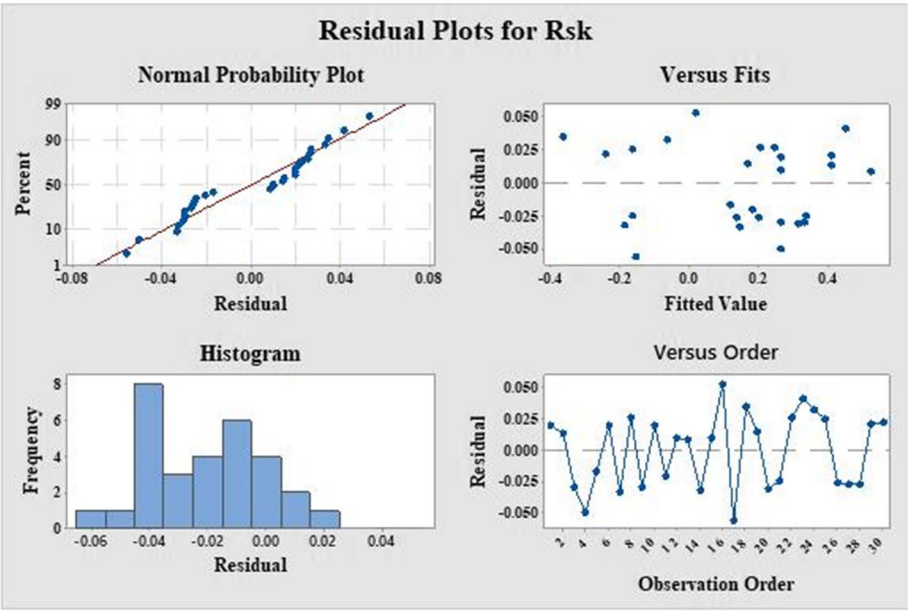

(c) Residual plots for surface skewness (Rsk)

Fig. 9 (continued)

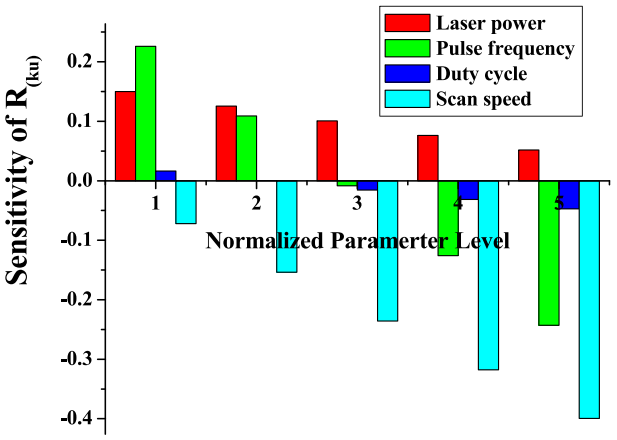

Fig. 10 Sensitivity plot for surface kurtosis (R_{ku})

distribution, which is greater than 4. The kurtosis value exhibits a decrease as the scan speed is increased. Bearing surfaces that are deemed appropriate typically exhibit a high kurtosis and a negative skew, as this is necessary to ensure the presence of flat regions that can facilitate low contact stresses as well as deep valleys that can serve as reservoirs for lubricant (Griffiths 2001).

The surface plot in Fig. 11a demonstrates the combined influence of pulse frequency and scan speed on surface kurtosis (R_{ku}). By maintaining a moderate pulse frequency

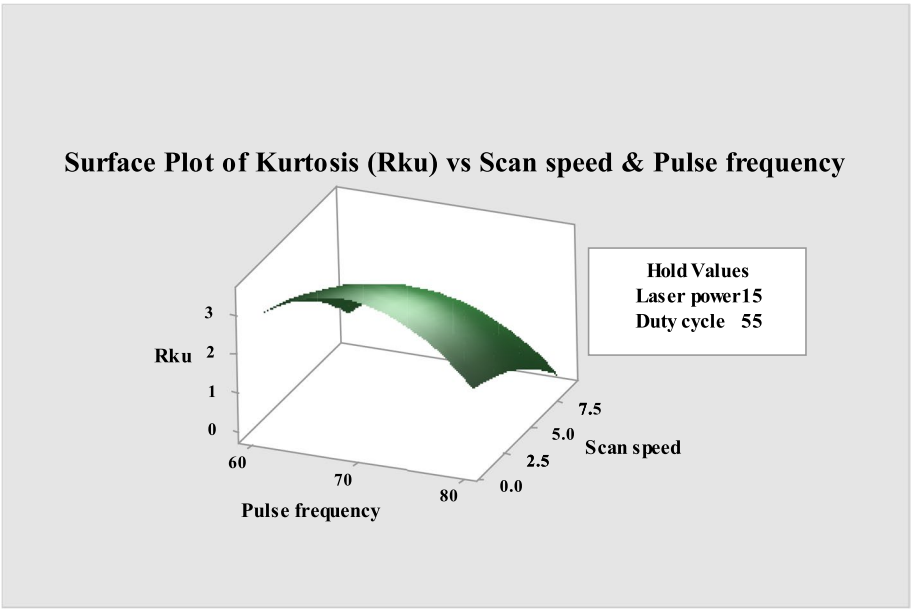

(a) Surface plot for surface kurtosis (R_{ku}) vs pulse frequency & scan speed

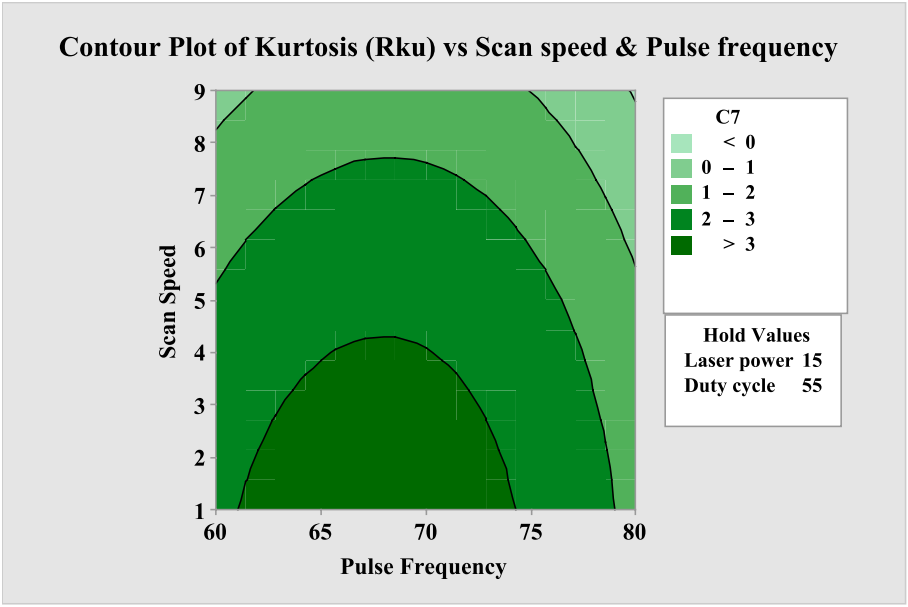

(b) Contour plot for surface kurtosis (R_{ku}) vs pulse frequency & scan speed

Fig. 11 **a** Surface plot for surface kurtosis (R_{ku}) vs pulse frequency and scan speed. **b** Contour plot for surface kurtosis (R_{ku}) vs pulse frequency and scan speed. **c** Residual plots for surface kurtosis (R_{ku})

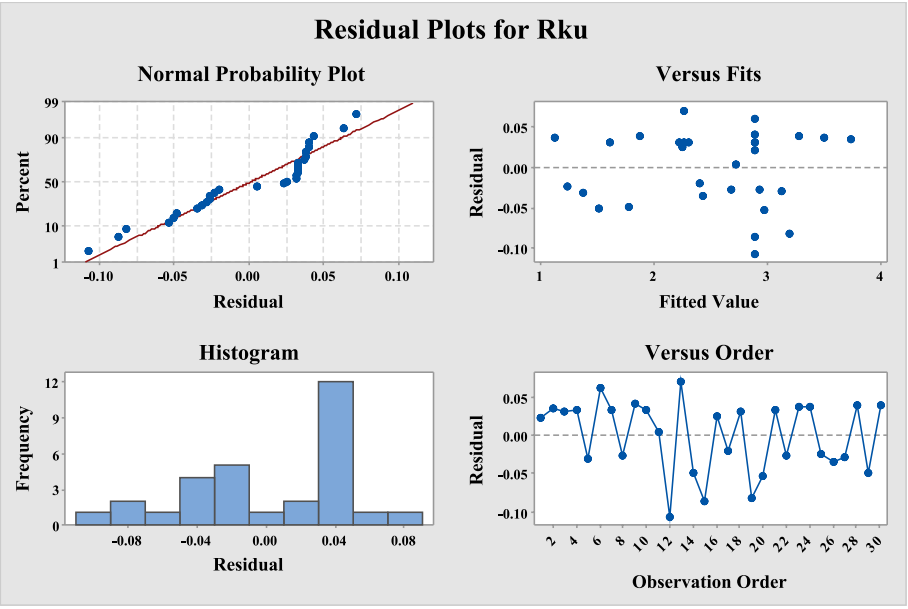

(c) Residual plots for surface kurtosis (R_{ku})

Fig. 11 (continued)

and a slower scan speed, one can achieve a higher level of kurtosis, which is desirable. When laser beam machining is used on nickel-based superalloys, such as Hastelloy C-276, it is observed that a moderate repetition rate may not provide sufficient ablation energy due to the longer period of heat dissipation. Conversely, a lower scan speed results in a longer irradiation time. Therefore, the desired ablation is accomplished by utilizing a low pulse frequency and low scan speed. This phenomenon facilitates the achievement of a desired level of surface smoothness, characterized by consistent peaks and valleys. The justification for the surface plot may be observed through the examination of the contour plot, specifically in Fig. 11b, which represents the surface kurtosis. The contour plots provide confirmation that the mathematical models established effectively characterize each dimension of texture.

It is common in the diagnostic analysis of variance (ANOVA) and response surface approaches to use residual plots, more specifically Figs. 7c, 9c and 11. The plots are utilized to evaluate the effectiveness of the proposed model and to analyze residual patterns. Typically, a non-uniform distribution pattern is noticed between the residual display and expected values. Based on the data presented, it can be noticed that the normal probability plot demonstrates a strong fit with regards to surface morphology, specifically in relation to roughness, skewness, and kurtosis. The presence of data clustering around the central axis suggests the potential viability of the constructed model.

Laser power, speed, scan spacing, and pulse duration are just a few of the variables that affect the surface roughness of laser-textured Hastelloy C276, among others. The aforementioned factors have the capability to modify the roughness characteristics of the surface, including Ra, R_{sk}, and R_{ku}. Consequently, these alterations have an impact on the contact area between the textured surface and the opposing surface that is in

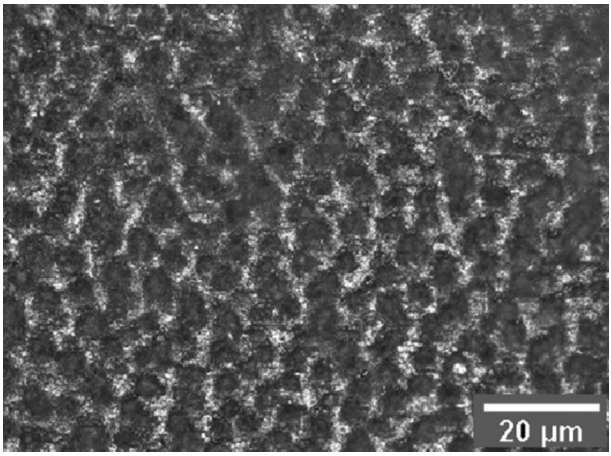

Fig. 12 Microscopic view of fiber laser textured surface

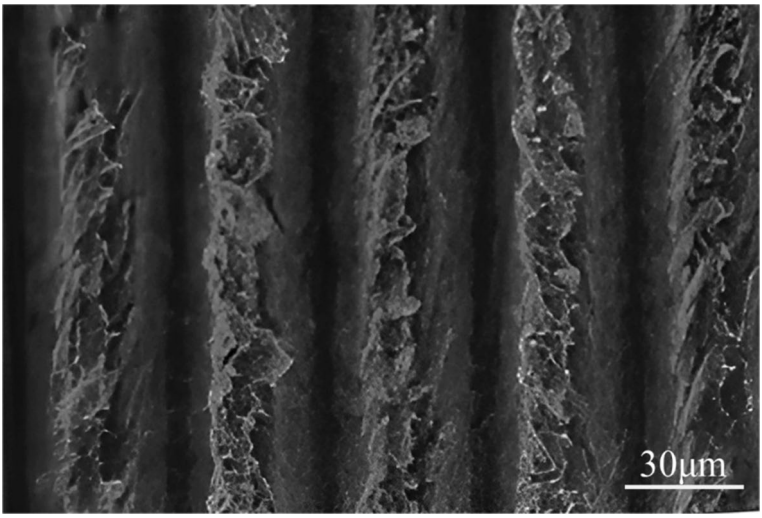

Fig. 13 SEM image of laser textured surface

contact. An increased roughness value corresponds to an augmented contact area and localized pressure, hence resulting in elevated frictional forces.

Figure 12 illustrates the microscopic examination of a non-uniformly textured surface under low laser power. Several studies have documented the occurrence of internal tensions during laser treatment, resulting from the alteration of local temperature. These tensions have the potential to penetrate the material at greater depths (Guarino et al. 2018).

The scanning electron microscopy (SEM) picture in Fig. 13 shows that the surface has almost perfectly symmetrical peaks and valleys, which supports both parametric and statistical analyses. The image also demonstrates that the re-solidification of molten debris occurs primarily over the peaks rather than the valleys, a phenomenon that the Gaussian energy distribution may help to explain. The presence of striation can be observed on the lateral surface of the produced grooves, exhibiting a distinct arrangement that corresponds to the trajectory of the laser beam. The aforementioned phenomenon arises as a result of

the dynamics of the melt pool along the laser's trajectory, and it also suggests the prevalence of the pyrolytic process.

In addition, the Fig. 14 depicts a microscopic examination conducted at a magnification of 50X, revealing the fiber laser-textured surface of Hastelloy C-276. The image provides insight into the manner in which molten materials flow within the textured surface. The interaction between a concentrated laser beam and the surface of Hastelloy C-276 conduces to the formation of a heat-affected zone characterised by high intensity. In this specific localised region, the material experiences an abrupt rise in temperature, resulting in its transition from a solid state to a liquid state (melting), followed by its conversion into vapours. The laser's intense energy induces the material to attain its melting point, facilitating its fluidity and subsequent formation of distinctive surface patterns. The observed effect is predominantly regulated by the key concepts of laser-material interactions, involving absorption, reflection, and thermal conductivity. The superalloy Hastelloy C-276 exhibits distinctive thermal and mechanical characteristics which exert an impact on the flow characteristics of molten material in laser-texturing techniques.

To provide evidence, let us explore the scientific instance of keyhole manufacturing within the context of laser welding. In laser welding, a similar process occurs, where the focused laser beam makes a deep depression (keyhole) in the material caused by high heating. The material found in the lowermost part of the keyhole reveals a state of molten matter, displaying a fluidic behaviour as it moves up the periphery and edge, eventually attaining a characteristic structure or shape. The observed phenomena have resemblance to the flow of molten material on laser-textured surfaces, hence offering a scientific foundation for comprehending the flow patterns that occur within the textured surface of Hastelloy C-276.

Furthermore, the direction as well as magnitude of molten material flow may be modified by a range of parameters, such as laser power, scanning speed, and pulse duration. The depth and width of textured patterns have been reported expand with higher power of the laser with slower scanning rates, hence influencing the flow behaviour of molten material. In addition, the selection of textured pattern geometry, such as grooves or bumps, may additionally impact the patterns of flow as well as topography of the surface.

Furthermore, the Figs. 15, 16 and 17 present surface roughness profiles obtained under various process parameter settings. In this particular scenario, the specified laser

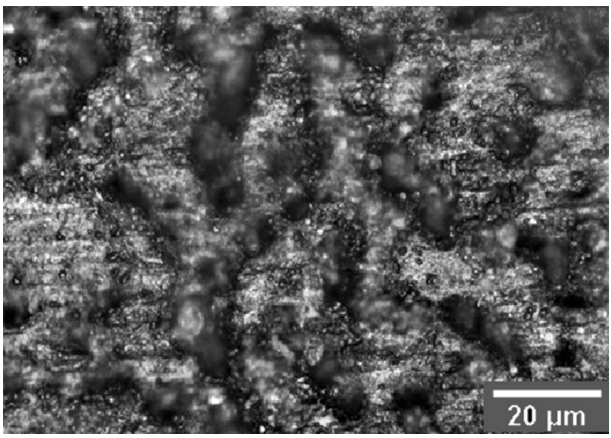

Fig. 14 Microscopic view of fiber laser textured surface

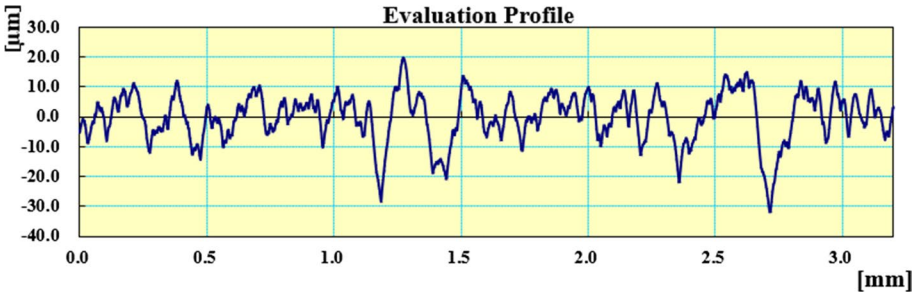

Fig. 15 Surface roughness profile at laser power of 15 W, pulse frequency of 70 kHz, duty cycle of 50%, and scan speed of 5 mm/s

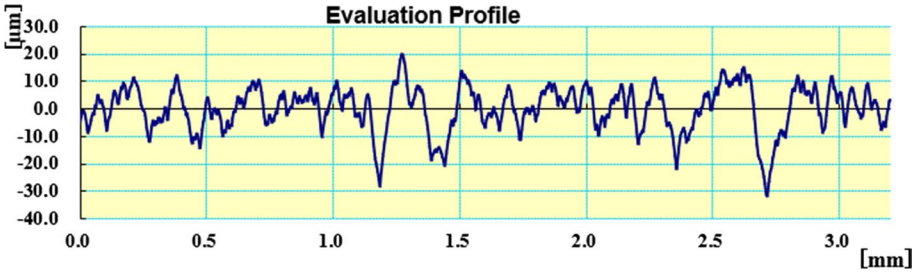

Fig. 16 Surface roughness profile at laser power of 10 W, pulse frequency of 70 kHz, duty cycle of 50%, and scan speed of 5 mm/s

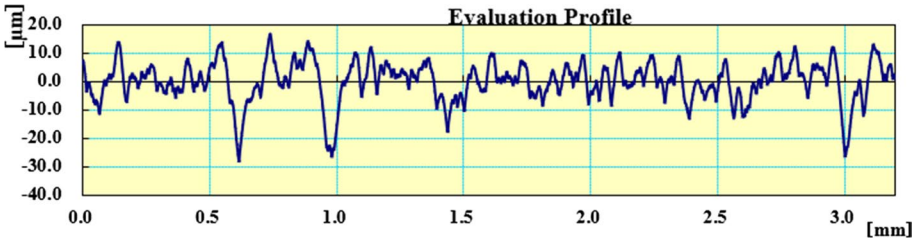

Fig. 17 Surface roughness profile at laser power of 15 W, pulse frequency of 70 kHz, duty cycle of 70%, and scan speed of 5 mm/s

parametric settings cause a distinct surface roughness profile. The specific energy input to the material is determined by the parameters of 15 W power, 70 kHz frequency, 50% duty cycle, and 5 mm/s scan speed. At the specified parameters, the laser's beam causes localised melting on the surface of Hastelloy C-276, which causes a removal of material as well as the formation of micro-grooves. The resultant surfaces pattern is influenced by the transverse overlapping distance of 7 µm between subsequent grooves/holes/channels/contour cavities, along with the overall number of 250 micro-grooves in a 5×5 cm^2 area.

In this Fig. 16, the laser power has been lowered to 10 W yet maintains the constancy of the remaining parameters. The drop in power has an impact on the energy input, resulting

in different material removal characteristics. The utilisation of a reduced power level in this instance leads to a reduction in material removal depth, resulting in micro-grooves that are possibly smoother when compared to those observed in the Fig. 15. The study of the influence of reduced power on surface roughness is a critical factor to take into consideration, as it offers valuable insight concerning the process's sensitivity to variations in power levels.

In this Fig. 17, the duty cycle is raised to 70% while remaining the laser power and frequency same. The duty cycle is an indicator that quantifies the percentage of the entire cycle duration in which the laser remains activated. An increased duty cycle corresponds to an extended period of laser irradiation on the surface of the material within each individual cycle. The prolonged duration of exposure could culminate in higher removal of material and modified surface texture characteristics.

The rise of duty cycle while retaining constant power and frequency might potentially lead to the formation of deeper grooves and perhaps change the surface roughness characteristics in comparison to Fig. 15. The rationale for investigating this parameter is in its effect on the rate at which material has removed and, consequently, on the roughness of the surface.

The 3D topology of the textured surface under the specified parametric conditions is depicted in Fig. 18. These conditions include a laser power of 10 W, a pulse frequency of 70 kHz, a duty cycle of 50%, and a scan speed of 5 mm/s. The region with a textured surface extends to a depth of up to 37.5 µm from the top face, spanning a length of 0.8 mm. The morphology of the textured profile of Hastelloy C-276 is significantly affected under these specified circumstances. The laser power of 10 watts is a determining factor in the quantity of energy that is imparted onto the surface. The presence of more force would give rise to a higher level of melting and vaporisation, hence causing the formation of uneven/irregular surface texture patterns. On the other hand, a reduced power level may not yield sufficient energy to cause the expected changes in the microstructure.

The pulse frequency of 70 kHz determines the quantity of laser pulses provided within a one-second interval. Raising the frequency of pulses facilitates a rise in

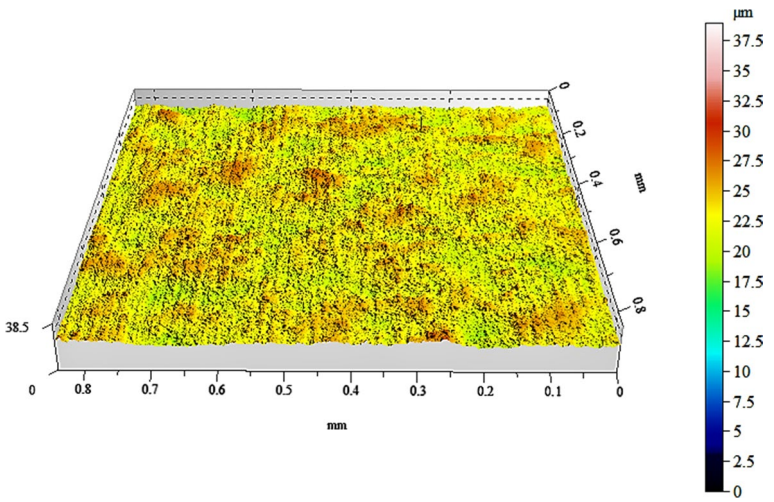

Fig. 18 3D topology of the textured profile of Hastelloy C-276

processing speed; yet, it is crucial to uphold an optimal equilibrium. Excessive frequency levels could culminate in the occurrence of overlapped pulses, hence impacting the overall quality of the texture. Conversely, a reduction in frequency may give rise to inadequate coverage, hence causing incomplete texturing.

The duty cycle of 50% signifies the proportion of the pulse duration to the pulse period. This parameter has an impact on the mean power transferred to the surface. The maintenance of a balanced duty cycle assures that the material has been provided with sufficient energy to undertake the process of texturing, yet additionally preventing the possibility of excessively heat generation that may potentially affect the integrity of its microstructure.

The pace at which the laser beam traverses the surface is determined by the scanning speed of 5 mm/s. A higher scanning speed can lead to a more refined surface quality as a consequence of less overlap among adjacent laser tracks. Nevertheless, an extremely raised velocity could potentially resulting in inadequate energy deposition, consequently impacting both the depth and quality of the textured surface.

The attainment for a textured surface with a depth of 37.5 µm from the top face across a length of 0.8 mm may be ascribed to the meticulous control of laser settings. The regulated manipulation of laser power, pulse frequency, duty cycle, and scan speed facilitate the precise ablation and subsequent re-solidification of the material, therefore attaining the envisioned microstructural modifications within the predetermined depth range.

3.2 Multi-objective optimization

Multi-objective optimization analysis is performed to achieve the target value of all three responses, i.e., R_a, R_{sk}, and R_{ku} of the fiber laser textured surface profile of Hastelloy C-276, based on the developed mathematical Eqs. (2), (3) and (4) are provided in Fig. 19.

The multi-objective optimization aims to achieve the target value arithmetical mean surface roughness of 1.2 µm along with a positive kurtosis value of 3. Besides, an optimized negative skewness value of − 0.350 is also aims for the utilization of the textured Hastelloy surface in bearing applications (Guarino et al. 2018). The negative skewness value of the considered surface suggests that surfaces have excellent fluid retention and lubricating properties. The surface with a positive value of skewness can wear off during high power applications. Multi-objective optimization results for the three responses are shown in Fig. 20. The current optimized parameter settings for achieving the target R_a (1.20 µm), R_{sk} (− 0.350), and R_{ku} (3) are laser power of 19.93 W, pulse frequency of 60 kHz, duty cycle of 38.96% along with scan speed of 8.41 mm/s.

Figure 20 shows the microscopic view of the textured surface on Hastelloy C-276 at the optimized machining condition at 50× magnification.

Figure 21 shows the AFM view of the textured surface on Hastelloy C-276 at the optimized machining condition. Optimized parametric settings helps to get adequate effective energy density at the line overlapping and spot overlapping instead of high laser fluence along the laser path. Thus, material removal has made uniformly throughout the overlapped area to form structure like honeycomb. Secondly the optimum parameter settings also help to eliminate the repeatability/ accuracy errors of movement by ball screw made X–Y axis of CNC based work station in laser machine. Thus, desired texture with precise surface topography can be achieved with low power fiber laser.

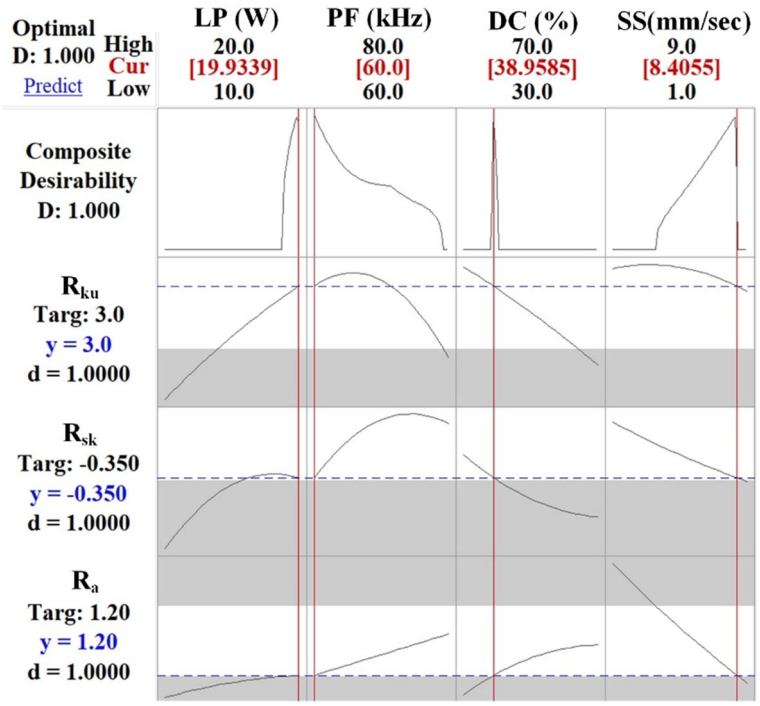

Fig. 19 Multi-objective optimization results for R_a, R_{sk}, and R_{ku}

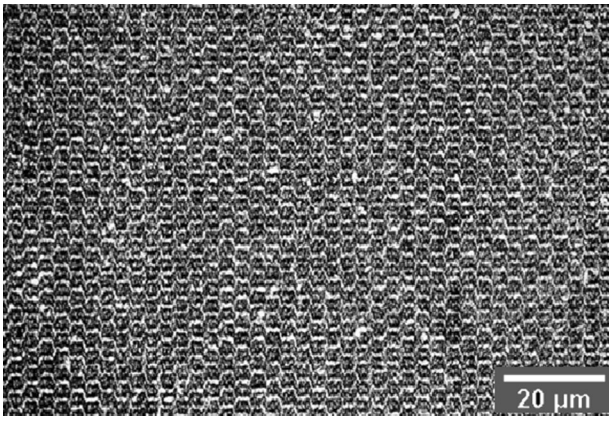

Fig. 20 Microscopic view of the textured surface on Hastelloy C-276 at optimized condition

3.3 Confirmation experiment

Confirmation experiments are conducted to validate the predicted results at the optimized experimental parameter settings. The mean prediction errors of the experimental values are evaluated to compare the experimental values of the three responses with their optimized values. The models developed are found to be an adequate representation of the experimental results as the prediction errors are less than 5%. A total of five confirmation experiments

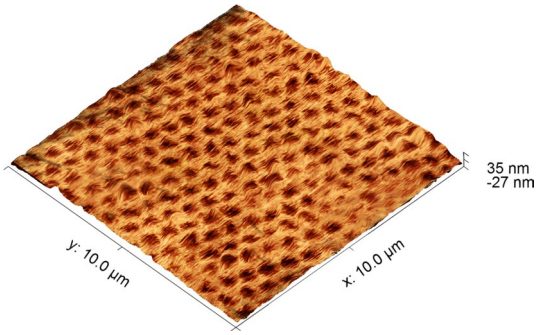

Fig. 21 AFM image of the textured surface on Hastelloy C-276 at optimized condition

are conducted. The experimental values of R_a, R_{sk}, and R_{ku} at optimized process parameter settings are shown in Table 4. The mean prediction errors for R_a, R_{sk}, and R_{ku} are found out to be within 3.41%, 4%, and 3.87% respectively. The calculated error values indicate that the produced results are very close agreement with the predicted results.

4 Conclusions

The present study employs fiber laser surface-texturing techniques as a cost-effective method compared to chemical etching and mechanical polishing for accurately texturing Hastelloy C-276 in order to achieve the desired surface properties. The utilisation of response surface methodology in this study provides the identification of the most favourable parameters for the fiber laser, leading to the achievement of consistent and dependable surface textures for the material.

The findings of the research work indicate that the desired surface roughness parameters (R_a, R_{sk}, and R_{ku}) of 1.2 m, − 0.35, and 3 are achieved by the utilisation of optimal process parameters, including laser power, pulse frequency, duty cycle, and scan speed. These values are determined to be suitable for applications involving bearings and high-power requirements. The results of the conformation tests further validate the efficacy and accuracy of our optimised parameters, as the errors for R_a, R_{sk}, and R_{ku} were found to be within 3.41%, 4%, and 3.87%, respectively.

The present study also reveals that the method employed exhibits superior cost-effectiveness, repeatability and precision compared to the existing techniques for achieving the specified surface attributes. The findings of the study also demonstrate the feasibility of employing textured surfaces made of Hastelloy C-276 in a diverse range of applications, particularly in the realms of bearings and high-power systems. The influence of surface roughness parameters on the contact area between the textured surface and the opposing surface in contact is a key factor to consider. This phenomenon leads to a decrease in the contact area and localised pressure, perhaps resulting in alterations to the frictional coefficient. The substantial level of agreement observed between our predictions and the empirical outcomes offers compelling support for the efficacy of the proposed approach. The findings of the study also indicate that the utilisation of textured surfaces offers distinct benefits compared to alternative approaches for surface treatment and that their applicability extends across several situations.

Table 4 Comparison between multi-objective optimization results with experimental results

Exp no.	R_a (μm)			R_{sk}			R_{ku}		
	Target value	Actual value at optimum condition	Percentage of errors	Target value	Actual value at optimum condition	Percentage of errors	Target value	Actual value at optimum condition (μm)	Percentage of errors
1	1.2	1.241	3.30	− 0.35	− 0.365	4.11	3	3.11	3.54
2	1.2	1.229	2.36	− 0.35	− 0.364	3.85	3	3.137	4.37
3	1.2	1.262	4.91	− 0.35	− 0.363	3.58	3	3.148	4.70
4	1.2	1.241	3.30	− 0.35	− 0.368	4.89	3	3.06	1.96
5	1.2	1.239	3.15	− 0.35	− 0.363	3.58	3	3.15	4.76
Mean Percentage of Errors (%) = 3.41				Mean Percentage of Errors (%) = 4			Mean Percentage of Errors (%) = 3.87		

The impacts of laser surface texturing on Hastelloy C-276 can be studied further in the future by taking into account additional responses such as wear rates, fatigue failure, and other mechanical properties such as hardness, tensile strength, etc.

The core objective of our work was to investigate the implications of various laser process parameters, such as laser power, pulse frequency, duty cycle, and scan speed, on the surface characteristics of Hastelloy C-276. Although the investigation encompassed the analysis of surface roughness (R_a), it should be noted that our study did not just revolve around this particular metric. Our objective was to conduct a thorough analysis of the surface morphology, specifically focusing on skewness (R_{sk}) and kurtosis (R_{ku}), along with roughness, in order to attain an in-depth comprehension of the broader topographical characteristics of the texture.

Additionally, in accordance with the research focus is concerned, the study's focus was comprehensive, embracing characteristics that expand beyond the merely consideration of roughness. The process of texturing Hastelloy C-276 was conducted with the objective of attaining customised surface characteristics suitable for high-power applications and bearings. The manipulation of surface texture has a substantial impact on multiple characteristics, including adhesion, wear resistance, frictional behaviour, and roughness. The intent of our investigation was to collectively optimise these characteristics in order to enhance the material's functionality for a wide range of applications.

The rationale for implementing surface texturing in this particular scenario was deemed essential due to several reasons.

1. *Wear Resistance*: The phenomenon of wear resistance is influenced by the modification of surface texture, which contributes to variations in the contact area and pressure distribution. These modifications have a substantial impact on the rates at which wear occurs. The objective of this study was to enhance the wear resistance of Hastelloy C-276 by optimising the parameters of surface texturing.
2. *Frictional behaviour*: The frictional behaviour of textured surfaces is frequently influenced by variations in surface topography. Minimising friction is of the utmost significance in high-power applications.
3. *Adhesion and Lubrication*: The technique of surface texturing has the potential to impact adhesion characteristics and enhance lubricating capabilities. The application of texturing techniques may culminate in distinct surface characteristics that have the potential to enhance the adhesion characteristics of materials and facilitate efficient retention of lubricants.

In our study, researchers conducted a comprehensive analysis of surface characteristics. In addition to examining surface roughness (R_a), researchers additionally laid emphasis on evaluating skewness (R_{sk}) and kurtosis (R_{ku}). Skewness offers valuable information on the level of gloss and luster exhibited by a surface, whereas kurtosis serves as an indicator of the degree of spikiness or bumpiness present on the surface. The comprehension of the material's overall texture quality serves as essential for the evaluation of its performance in numerous applications, including bearings. These criteria play a fundamental role in this knowledge.

The primary objective of surface texturing, within the scope of this investigation, is to enhance the characteristics of Hastelloy C-276, a superalloy, with the aim of optimising its suitability for certain applications, such as bearings and high-power systems. The objective of surface texturing is to enhance multiple characteristics like as adhesion, friction, wear

resistance, surface area, and wettability. This study primarily centers on the attainment employing specified surface roughness parameters (R_a, R_{sk}, and R_{ku}) by means of fibre laser surface texturing utilised on Hastelloy C-276. This investigation seeks at addressing the gap in existing research by exploring the optimisation of laser process parameters for the specific material under consideration. The objective is to enable cost-effective utilisation of this material in high-power applications.

In addition, and in context with the methodology and experimental Design are concerned, the present work utilises RSM and CCD to systematically investigate the implications of laser power, pulse frequency, duty cycle, and scan speed on surface parameters, namely Ra, Rsk, and Rku. The second-order polynomial models that have been generated have statistical significance, as demonstrated by the ANOVA findings presented in Table 3. Furthermore, these models have been confirmed by confirmation experiments, as indicated in Table 4, which demonstrate a notable level of accuracy and repeatability.

Moreover, in accordance with the examination of sensitivity analysis and physical mechanisms is concerned, the sensitivity analyses displayed in Eqs. 5–16 illustrate the complex interdependencies or relationships among process parameters and surface characteristics. The article explores the underlying principles of these relationships from a physics perspective, elucidating phenomena such as Marangoni-driven flow, capillary waves, and hydrothermal waves. This study delves into the intricate relationship among laser power, scan speed, pulse frequency, and duty cycle, providing a comprehensive analysis of how these variables impact surface roughness, skewness, and kurtosis.

The topic of interest in this study is multi-objective optimisation and its experimental validation.

The utilisation of multi-objective optimisation techniques is employed in order to attain specific target values for surface roughness characteristics, hence assuring the suitableness of Hastelloy C-276 for applications involving high levels of power. The optimised parameters undergo validation through confirmation studies, displaying an excellent correlation among anticipated and experimental values (with an error range of 3.41% to 4%). The aforementioned validation highlights the accuracy of the developed models and the efficacy of the optimisation procedure.

In this article, we will discuss the potential future directions and implications of the topic at hand.

The article offers prospective directions for future research, which encompass the investigation of additional characteristics like as wear rates, fatigue failure, hardness, and tensile strength. Additional investigation into the implications of laser surface texturing on the aforementioned attributes would contribute to an improved understanding of the behaviour of Hastelloy C-276 under varying circumstances.

In summary, this research provides a thorough examination of the fibre laser surface texturing technique used to Hastelloy C-276, offering insights into the fundamental principles and optimisation methodologies involved. The present study not only addresses a significant void in the current body of literature nevertheless presents a rigorous approach for enhancing surface characteristics. The findings provide significant contributions to the enhancement of Hastelloy C-276 for high-power applications, highlighting the significance of surface texturing in customising material characteristics.

In essence, the objective of this research was to thoroughly enhance the surface characteristics of Hastelloy C-276. The process of surface texturing was conducted with the aim of attaining certain attributes that go beyond mere roughness. These properties encompass higher wear resistance, modified frictional characteristics, enhanced adhesion, and superior lubrication. The goal was to get a comprehensive knowledge of the

influence of laser process parameters on material performance throughout various high-power applications and bearing scenarios by examining numerous surface attributes. The optimisation of these characteristics played a crucial part in customising the material to meet specific industrial demands, therefore providing a significant contribution to the area of materials science and engineering.

Acknowledgements The authors extend their appreciation to the Deanship of Scientific Research at King Khalid University (KKU) for funding this research through the Research Group Program under the Grant Number: (R.G.P.2/572/44).

Author contributions Conceptualization, AS, DP, NR, AMM, PSG, SS; formal analysis, AS, DP, NR, AMM, PSG, SS; investigation, AS, DP, NR, AMM, PSG, SS; writing—original draft preparation, AS, DP, NR, AMM, PSG, SS; writing—review and editing, SS, SHK, CL, HS, MA; supervision, SS, SHK, CL, HS, MA; project administration, SS, SHK, CL, HS, MA; funding acquisition, SS, MA. All authors have read and agreed to the published version of the manuscript.

Funding The authors extend their appreciation to the Deanship of Scientific Research at King Khalid University (KKU) for funding this research through the Research Group Program under the Grant Number: (R.G.P.2/572/44).

Data availability The data that support the findings of this study are available within the manuscript.

Declarations

Conflict of interest The authors declare that they have no conflict of interest.

Ethical approval Not applicable.

Consent to participate Not applicable.

Consent to publish All authors have read and approved this manuscript.

References

Aggarwal, V., Pruncu, C.I., Singh, J., Sharma, S., Pimenov, D.Y.: Empirical investigations during WEDM of Ni-27Cu-3.15Al-2Fe-1.5Mn based superalloy using response surface methodology for high temperature corrosion resistance applications. Materials **13**, 3470 (2020). https://doi.org/10.3390/ma13163470

Al-Falahi, M., Fadaeifard, F., Al-Falahi, M.D.A., Bin Baharudin, B.T.H.T., Hong, T.S.: Surface damages and tool wear mode in end milling of Hastelloy-C276 under dry and wet conditions. Mater. Sci. Eng. Technol. **47**(12), 1182–1192 (2016)

Al-Tameemi, H.A., Al-Dulaimi, T., Awe, M.O., Sharma, S., Pimenov, D.Y., Koklu, U., Giasin, K.: Evaluation of cutting-tool coating on the surface roughness and hole dimensional tolerances during drilling of Al6061-T651 alloy. Materials **14**(7), 1783 (2021). https://doi.org/10.3390/ma14071783

Cui, X., Li, C., Zhang, Y., Ding, W., An, Q., Liu, B., Li, H.N., Said, Z., Sharma, S., Li, R., Debnath, S.: A comparative assessment of force, temperature and wheel wear in sustainable grinding aerospace alloy using bio-lubricant. Front. Mech. Eng. **18**(2), 3 (2022a). https://doi.org/10.1007/s11465-022-0719-x

Cui, X., Li, C., Zhang, Y., Said, Z., Debnath, S., Sharma, S., Ali, H.M., Yang, M., Gao, T., Li, R.: Grindability of titanium alloy using cryogenic nanolubricant minimum quantity lubrication. J. Manuf. Process. **80**, 273–286 (2022b). https://doi.org/10.1016/j.jmapro.2022.06.003

Davis, J.R.: Nickel, Cobalt, and Their Alloys. ASM International, Materials Park (2000)

Dikshit, M.K., Singh, S., Pathak, V.K., Saxena, K.K., Agrawal, M.K., Malik, V., Khan, M.I.: Surface characteristics optimization of biocompatible Ti_6Al_4V with RCCD and NSGA II using die sinking EDM. J. Market. Res. **24**, 223–235 (2023). https://doi.org/10.1016/j.jmrt.2023.03.005

Duan, Z., Li, C., Zhang, Y., Yang, M., Gao, T., Liu, X., Li, R., Said, Z., Debnath, S., Sharma, S.: Mechanical behavior and semiempirical force model of aerospace aluminum alloy milling using nano biological lubricant. Front. Mech. Eng. (2022). https://doi.org/10.1007/s11465-022-0720-4

Dwivedi, S.P., Chaudhary, V., Sharma, S.: Effect of the addition of waste glass powder along with TiC as reinforcement on microstructure, wettability, mechanical and tribological behavior of AZ91D magnesium based alloy. Int. J. Metal Cast. (2023). https://doi.org/10.1007/s40962-023-01117-3

Georges, C., Semmar, N., Boulmer-Leborgne, C.: Effect of pulsed laser parameters on the corrosion limitation for electric connector coatings. Opt. Lasers Eng. **44**(12), 1283–1296 (2006)

Gordani, G.R., ShojaRazavi, R., Hashemi, S.H., Isfahani, A.R.N.: Laser surface alloying of an electroless Ni–P coating with Al-356 substrate. Opt. Lasers Eng. **46**(7), 550–557 (2008)

Griffiths, B.: Manufacturing Surface Technology: Surface Integrity and Functional Performance. CRC Press, Cambridge (2001)

Guarino, S., Ponticelli, G.S., Giannini, O., Genna, S., Trovalusci, F.: Laser milling of yttria-stabilized zirconia by using a Q-switched Yb: YAG fiber laser: experimental analysis. Int. J. Adv. Manuf. Technol. **94**(1), 1373–1385 (2018)

Hashim, M., Babu, K.S.R., Duraiselvam, M., Natu, H.: Improvement of wear resistance of Hastelloy C-276 through laser surface melting. Mater. Des. **46**, 546–551 (2013)

Horváth, R., Czifra, Á., Drégelyi-Kiss, Á.: Effect of conventional and non-conventional tool geometries to skewness and kurtosis of surface roughness in case of fine turning of aluminium alloys with diamond tools. Int. J. Adv. Manuf. Technol. **78**(1), 297–304 (2015)

Jia, D., Zhang, Y., Li, C., Yang, M., Gao, T., Said, Z., Sharma, S.: Lubrication-enhanced mechanisms of titanium alloy grinding using lecithin biolubricant. Tribol. Int. (2022). https://doi.org/10.1016/j.triboint.2022.107461

Khan, A.M., Anwar, S., Alfaify, A., et al.: Comparison of machinability and economic aspects in turning of Haynes-25 alloy under novel hybrid cryogenic-LN oils-on-water approach. Int. J. Adv. Manuf. Technol. (2022). https://doi.org/10.1007/s00170-022-08815-y

Khan, M., Shah, F., Abdullaev, S., Li, S., Altuijri, R., Vaidya, H., Khan, A.: Heat and mass transport behavior in bio-convective reactive flow of nanomaterials with Soret and Dufour characteristics. Case Stud. Therm. Eng. **49**, 103347 (2023). https://doi.org/10.1016/j.csite.2023.103347

Kibria, G., Sen, A., Tariq Aziz, H.M., Doloi, B., Bhattacharyya, B.: Pulsed Nd: YAG laser surface texturing of pure titanium material. In: Precision Product-Process Design and Optimization, pp. 361–390. Springer, Singapore (2018)

Kiranakumar, V., Ramakrishnaiah, T., Naveen, S., Khan, M., Gunderi, P., Reddy, S., Oreijah, M., Guedri, K., Bafakeeh, O., Jameel, M.: A review on electrical and gas-sensing properties of reduced graphene oxide–metal oxide nanocomposites. Biomass Convers. Biorefin. (2022). https://doi.org/10.1007/s13399-022-03258-7

Kumar, R., Dwivedi, R., Arya, R., Sonia, P., Yadav, A., Saxena, K., Khan, M., Ben Moussa, S.: Current development of carbide free bainitic and retained austenite on wear resistance in high silicon steel. J. Mater. Res. Technol. (2023a). https://doi.org/10.1016/j.jmrt.2023.05.067

Kumar, Y., Hussain, S., Kodi, R., Ali, F., Guedri, K., Eldin, S., Khan, M.: Numerical analysis of magneto-hydrodynamics Casson nanofluid flow with activation energy, Hall current and thermal radiation. Sci. Rep. (2023b). https://doi.org/10.1038/s41598-023-28379-5

Kumar, M.S., Sathisha, N., Manjnatha, S., et al.: Fatigue surface analysis of AL A356 alloy reinforced hematite metal matrix composites. Biomass Convers. Biorefin. (2023c). https://doi.org/10.1007/s13399-023-04634-7

Lashin, M.M.A., Ibrahim, M.Z., Khan, M.I., Guedri, K., Saxena, K.K., Eldin, S.M.: Fuzzy control modeling to optimize the hardness and geometry of laser cladded Fe-based MG single track on stainless steel substrate prepared at different surface roughness. Micromachines **13**(12), 2191 (2022). https://doi.org/10.3390/mi13122191

Lin, B., Liu, R., Jia, Q., Cui, Y., Yang, R.: Effect of surface topography on room temperature tensile ductility of TiAl. JOM **69**(12), 2583–2587 (2017)

Liu, M., Li, C., Yang, M., Gao, T., Wang, X., Cui, X., Zhang, Y., Said, Z., Sharma, S.: Mechanism and enhanced grindability of cryogenic air combined with biolubricant grinding titanium alloy. Tribol. Int. **187**, 108704 (2023). https://doi.org/10.1016/j.triboint.2023.108704

Ma, G., Wu, D., Guo, D.: Segregation characteristics of pulsed laser butt welding of Hastelloy C-276. Metall. Mater. Trans. A **42**(13), 3853–3857 (2011)

Mohammed, M.K., Umer, U., Al-Ahmari, A.: Optimization of laser micro milling of alumina ceramic using radial basis functions and MOGA-II. Int. J. Adv. Manuf. Technol. **91**(5), 2017–2029 (2017)

Prasanthi, P., Kumar, M., Mallampati, S., Madhav, V., Saxena, K., Mohammed, K., Khan, M., Upadhyay, G., Eldin, S.: Mechanical properties of carbon fiber reinforced with carbon nanotubes and graphene filled

epoxy composites: experimental and numerical investigations. Mater. Res. Express (2023). https://doi.org/10.1088/2053-1591/acaef5
Roy, A., Manna, I.: Laser surface engineering to improve wear resistance of austempered ductile iron. Mater. Sci. Eng. A **297**(1–2), 85–93 (2001)
Sarker, A., Tran, N., Rifai, A., Elambasseril, J., Brandt, M., Williams, R., et al.: Angle defines attachment: switching the biological response to titanium interfaces by modifying the inclination angle during selective laser melting. Mater. Des. **154**, 326–339 (2018)
Sehar, B., Waris, M., Gilani, S., Ansari, U., Mushtaq, S., Khan, N., Jameel, M., Khan, M., Bafakeeh, O., Eldin, S.: The impact of laminations on the mechanical strength of carbon-fiber composites for prosthetic foot fabrication. Crystals **12**, 1429 (2022). https://doi.org/10.3390/cryst12101429
Shahid, M., Javed, H.M.A., Ahmad, M., Qureshi, A., Khan, M., Alnuwaiser, M., Ahmed, A., Khan, M., Eldin, S., Shahid, A., Rafique, A.: A brief assessment on recent developments in efficient electrocatalytic nitrogen reduction with 2D non-metallic nanomaterials. Nanomaterials (2022). https://doi.org/10.3390/nano12193413
Singh, J., Gill, S.S., Dogra, M., Singh, R., Singh, M., Sharma, S., Singh, G., Li, C., Rajkumar, S.: State of the art review on the sustainable dry machining of advanced materials for multifaceted Engineering applications: progressive advancements and directions for future prospects. Mater. Res. Express (2022). https://doi.org/10.1088/2053-1591/ac6fba
Singh, J., Gill, S.S., Dogra, M., Sharma, S., Singh, M., Dwivedi, S.P., Li, C., Singh, S., Muhammad, S., Salah, B., et al.: Effect of Ranque–Hilsch vortex tube cooling to enhance the surface-topography and tool-wear in sustainable turning of Al-5.6Zn-2.5Mg-1.6Cu-0.23Cr-T6 aerospace alloy. Materials **15**, 5681 (2022a). https://doi.org/10.3390/ma15165681
Singh, G., Aggarwal, V., Singh, S., Singh, B., Sharma, S., Singh, J., Li, C., Ilyas, R.A., Mohamed, A.: Experimental investigation and performance optimization during machining of Hastelloy C-276 using green lubricants. Materials **15**(15), 5451 (2022b). https://doi.org/10.3390/ma15155451
Singh, G., Kumar, H., Kansal, H.K., Sharma, K., Kumar, R., Chohan, J.S., Singh, S., Sharma, S., Li, C., Królczyk, G., Królczyk, J.B.: Multiobjective optimization of chemically assisted magnetic abrasive finishing (MAF) on Inconel 625 tubes using genetic algorithm: modeling and microstructural analysis. Micromachines **13**(8), 1168 (2022c). https://doi.org/10.3390/mi13081168
Singh, G., Sharma, S., Seikh, A.H., Li, C., Zhang, Y., Rajkumar, S., Kumar, A., Singh, R., Eldin, S.M.: A novel study on the influence of graphene-based nanofluid concentrations on the response characteristics and surface-integrity of Hastelloy C-276 during minimum quantity lubrication. Heliyon (2023a). https://doi.org/10.1016/j.heliyon.2023.e19175
Singh, B., Kumar, I., Saxena, K., Mohammed, K., Khan, M., Ben Moussa, S., Abdullaev, S.: A future prospects and current scenario of aluminium metal matrix composites characteristics. Alex. Eng. J. **76**, 1–17 (2023b). https://doi.org/10.1016/j.aej.2023.06.028
Singh, G., Sehijpal, S., Sharma, S., Singh, J., Li, C., Krolczyk, G., Kumar, A., Eldin, S.: Performance investigations for sustainability assessment of Hastelloy C-276 under different machining environments. Heliyon **9**, e13933 (2023c). https://doi.org/10.1016/j.heliyon.2023.e13933
Soveja, A., Cicală, E., Grevey, D., Jouvard, J.M.: Optimisation of TA6V alloy surface laser texturing using an experimental design approach. Opt. Lasers Eng. **46**(9), 671–678 (2008)
Sun, S., Khan, M.I., Al-Khaled, K., Raza, A., Abdullaev, S.S., Khan, S.U., Eldin, S.M.: Prabhakar fractional approach for enhancement of heat transfer due to hybrid nanomaterial with sinusoidal heat conditions. Case Stud. Therm. Eng. **49**, 103240 (2023). https://doi.org/10.1016/j.csite.2023.103240
Syreyshchikova, N.V., Pimenov, D.Y., Gupta, M.K., Nadolny, K., Giasin, K., Aamir, M., Sharma, S.: Relationship between pressure and output parameters in belt grinding of steels and nickel alloy. Materials **14**(16), 4704 (2021a). https://doi.org/10.3390/ma14164704
Syreyshchikova, N.V., Pimenov, D.Y., Gupta, M.K., Nadolny, K., Giasin, K., Sharma, S.: Establishing the relationship between cutting speed and output parameters in belt grinding on steels, aluminum and nickel alloys: development of recommendations. Materials **14**, 1974 (2021b). https://doi.org/10.3390/ma14081974
Vemanaboina, H., Babu, M.M., Prerana, I.C., Gundabattini, E., Yelamasetti, B., Saxena, K.K., Agrawal, M.K.: Evaluation of residual stresses in CO_2 laser beam welding of SS316L weldments using FEA. Mater. Res. Express **10**(1), 016509 (2023). https://doi.org/10.1088/2053-1591/acb0b5
Watson, W., Spedding, T.A.: The time series modelling of non-Gaussian engineering processes. Wear **83**(2), 215–231 (1982)
Xing, Y., Deng, J., Feng, X., Yu, S.: Effect of laser surface texturing on Si_3N_4/TiC ceramic sliding against steel under dry friction. Mater. Des. **1980–2015**(52), 234–245 (2013)
Xu, W., Li, C., Zhang, Y., Ali, H.M., Sharma, S., Li, R., Yang, M., Gao, T., Liu, M., Wang, X., Said, Z., Liu, X., Zhou, Z.: Electrostatic atomization minimum quantity lubrication machining: from

mechanism to application. Int. J. Extreme Manuf. (2022). https://doi.org/10.1088/2631-7990/ac9652

Xu, W., Li, C., Cui, X., Zhang, Y., Yang, M., Gao, T., Liu, M., Wang, X., Zhou, Z., Sharma, S., Dambatta, Y.S.: Atomization mechanism and machinability evaluation with electrically charged nanolubricant grinding of GH4169. J. Manuf. Process. **106**, 480–493 (2023). https://doi.org/10.1016/j.jmapro.2023.10.037

Yilbas, B.S., Ali, H.: Laser texturing of Hastelloy C276 alloy surface for improved hydrophobicity and friction coefficient. Opt. Lasers Eng. **78**, 140–147 (2016)

Authors and Affiliations

Abhisekh Sen[1] · Debal Pramanik[2] · Nilanjan Roy[2] · Ahmed Mohammed Mahmood[3] · Partha Sarthi Ghosh[1] · Shubham Sharma[4,5,6] · Saja Hameed Kareem[7] · Changhe Li[7] · Hayder Sharif[8] · Mohamed Abbas[9]

✉ Shubham Sharma
shubham543sharma@gmail.com; shubhamsharmacsirclri@gmail.com

Abhisekh Sen
abhishek.sen1986@gmail.com

Debal Pramanik
debpramanik18@yahoo.com

Nilanjan Roy
nilanjan_83@yahoo.co.in

Ahmed Mohammed Mahmood
ahmed.m53@alnoor.edu.iq

Partha Sarthi Ghosh
psghosh1991@gmail.com

Saja Hameed Kareem
saja.kareem@nust.edu.iq

Changhe Li
sy_lichanghe@163.com

Hayder Sharif
haydershrf@gmail.com

Mohamed Abbas
mabas@kku.edu.sa

[1] Department of Mechanical Engineering, Calcutta Institute of Technology, Howrah 711316, India

[2] Department of Mechanical Engineering, Swami Vivekananda Institute of Science and Technology, Kolkata 700145, India

[3] Department of Optical Techniques, Al-Noor University College, Nineveh, Iraq

[4] Department of Mechanical Engineering, University Centre for Research and Development (UCRD), Chandigarh University, Mohali, India

[5] School of Mechanical and Automotive Engineering, Qingdao University of Technology, Qingdao 266520, China

[6] Department of Mechanical Engineering, Lebanese American University, Kraytem, Beirut 1102-2801, Lebanon

[7] National University of Science and Technology, Nasiriyah, Dhi Qar, Iraq

[8] Medical Technical College, Al-Farahidi University, Baghdad, Iraq

[9] Electrical Engineering Department, College of Engineering, King Khalid University, 61421 Abha City, Saudi Arabia